Global and Planetary Change 242 (2024) 104533

Contents lists available at ScienceDirect

Global and Planetary Change

journal homepage: www.elsevier.com/locate/gloplacha

Heterogeneous marine response during the Toarcian Oceanic Anoxic Event (TOAE): The potential role of storminess

Yuzhu Ge [a,b], Zhong Han [a,b,*], Thomas J. Algeo [a,c,d,e,*], David B. Kemp [c], Luya Wu [f]

[a] State Key Laboratory of Oil and Gas Reservoir Geology and Exploitation, Chengdu University of Technology, Chengdu 610059, China
[b] Institute of Sedimentary Geology & Key Laboratory of Deep-Time Geography & Environmental Reconstruction and Application of Ministry of Natural Resources, Chengdu University of Technology, Chengdu 610059, China
[c] State Key Laboratory of Biology and Environmental Geology and Hubei Key Laboratory for Critical Zone Evolution, School of Earth Sciences, China University of Geoscience, Wuhan, Hubei 430074, China
[d] State Key Laboratory of Geological Processes and Mineral Resources, China University of Geosciences, Wuhan, Hubei 430074, China
[e] Department of Geosciences, University of Cincinnati, Cincinnati, OH 45221-0013, USA
[f] Research Institute of Petroleum Exploration and Development, PetroChina Southwest Oil and Gas Field Company, Chengdu, Sichuan 610051, China

ARTICLE INFO

Editor: Dr. Maoyan Zhu

Keywords:
Jurassic
Tempestite
Pycnocline
Stratification
Redox
Productivity

ABSTRACT

The Toarcian Oceanic Anoxic Event (TOAE; ~183 Ma) represents an important hyperthermal and deoxygenation event in the Early Jurassic. However, TOAE marine records are spatially heterogeneous with regard to nutrient levels, primary productivity, redox conditions and organic enrichment. This non-uniform response to global hyperwarming is not readily accounted for by local variations in paleogeography, climate, or water depth. Largely overlooked to date is the intensified storm activity that characterized the TOAE, and the role that this may have played in controlling marine responses to that event. A review of TOAE studies from multiple marine environments suggests that storm intensity covaried with paleoceanographic conditions, such as nutrient availability, primary productivity, redox conditions, and organic-rich sedimentation. At mid-paleolatitude sites, relatively weak storm activity during the TOAE induced short-term watermass oxygenation, and marine settings were mainly characterized by enhanced anoxia (even euxinia), water-column stratification, increased primary productivity (fueled by terrestrial runoff and P regeneration in euxinic settings), and organic-rich sedimentation. At low-paleolatitude sites, TOAE storm activity was relatively strong, and contributed to marine environments characterized by oxic to suboxic conditions, reduced water-column stratification, decreased primary productivity (possibly due to limited P regeneration and upwelling), low sedimentary organic content, and locally high oolite abundance. TOAE marine sites at all paleolatitudes exhibit: i) sea-level rise and enhanced continental weathering fluxes linked to an intensified hydrological cycle; ii) reduced dinoflagellate and increased cyanobacterial activity; and iii) low $\delta^{15}N$ values (mainly −1‰ to +3‰) linked to enhanced diazotrophic nitrogen fixation. The spatial heterogeneity of the response of TOAE marine systems is difficult to reconcile with scenarios linking increased terrestrial flux to marine eutrophication, primary productivity increase and organic-rich sedimentation. Consequently, we hypothesize that the intensity of storm activity influenced TOAE marine systems, and that this factor can, at least partially, account for heterogeneous patterns of environmental changes at middle versus low paleolatitudes and open versus restricted marine settings. Importantly, increased storm activity can induce pycnocline deepening via vertical water-column mixing, thereby promoting: i) enhanced aerobic degradation of organic matter (low sediment organic matter content) due to a reduced oxygen-minimum zone; ii) less nutrient upwelling from deep waters into the photic zone (nutrient-depleted upper ocean), and iii) blooms of nitrogen-fixing cyanobacteria (low $\delta^{15}N$) and calcification (ooid formation). Thus, the interaction between storminess and pycnocline depth is a potentially important factor affecting marine environmental changes during TOAE. These findings have implications for modern oceans now experiencing climatic warming and intensified tropical storm activity.

* Corresponding authors at: State Key Laboratory of Oil and Gas Reservoir Geology and Exploitation, Chengdu University of Technology, Chengdu 610059, China.
E-mail addresses: hanzhong19@cdut.edu.cn (Z. Han), thomas.algeo@uc.edu (T.J. Algeo).

https://doi.org/10.1016/j.gloplacha.2024.104533
Received 21 March 2024; Received in revised form 16 June 2024; Accepted 24 July 2024
Available online 28 July 2024

1. Introduction

The Early Jurassic Toarcian Oceanic Anoxic Event (TOAE; ca. 183 Ma) coincided with climate upheaval characterized by high atmospheric CO_2, enhanced continental weathering and terrigenous fluxes, sea-level rise, ocean deoxygenation and organic-rich sedimentation (Jenkyns, 2010; Brazier et al., 2015; Krencker et al., 2015; Them et al., 2017a, 2017b; Han et al., 2018; Remírez and Algeo, 2020a; Kemp et al., 2022a; Yan et al., 2023). The TOAE also experienced strong climatic warming and carbon cycle disturbance. Globally, the event is marked in the sedimentary record by a negative carbon-isotope excursion (NCIE) that is universally found in both inorganic and organic material from terrestrial and marine strata. The probable ultimate trigger of the TOAE was emplacement and eruption of the Karoo-Ferrar Large Igneous Province (KFLIP) (Percival et al., 2015; Font et al., 2022; Ware et al., 2023).

It has been long recognized that marine paleoenvironmental changes during the TOAE were spatially heterogeneous (Wignall et al., 2005; Caruthers et al., 2014; Baroni et al., 2018; Fantasia et al., 2018a; Remírez and Algeo, 2020a; Kemp et al., 2022a; Chen et al., 2023). For example, total organic content (TOC) varies from 0.1% to >10%, and reported marine redox conditions range from anoxic (even euxinic) to oxic facies at different localities. Continental chemical weathering shows both increases and decreases at different sites (e.g., McArthur et al., 2008; Fantasia et al., 2018a; Kemp et al., 2019).

Previous studies have proposed local paleogeographic controls (such as basinal restriction) and climatic conditions (humid vs. arid) as causes for heterogenous marine TOAE responses (e.g., McArthur et al., 2008; Baroni et al., 2018; Fantasia et al., 2018b; Remírez and Algeo, 2020a; Fu et al., 2021). However, the relation between heterogenous marine responses and local paleogeographic and climatic conditions is unclear. For example, organic-rich and anoxic facies have been found in both restricted and open marine settings (e.g., McArthur et al., 2008; Kemp et al., 2022a, 2022b). In the same climate belt, marine redox conditions vary from oxic to anoxic conditions (e.g., McArthur et al., 2008; Kemp and Izumi, 2014). In addition, TOAE sections from different paleogeographic settings and climate belts display a range of primary productivity conditions, but all record low $\delta^{15}N$ values (mainly −1‰ to +3‰) (Jenkyns et al., 2001; Ruebsam et al., 2018; Kemp et al., 2019; Wang et al., 2021).

Storminess is a prominent feature of TOAE marine records (Suan et al., 2013; Han et al., 2018; Izumi et al., 2018; Xu et al., 2018). In general, the intensity of storm activity is strongly influenced by mean global temperature, with greater storm intensity (specifically tropical cyclone intensity) linked to hyperwarming (Krencker et al., 2015; Yan et al., 2023). This relationship exists because warming of the ocean-surface layer permits greater transfer of latent energy to the atmosphere through evaporation (Donnelly et al., 2015; Yan et al., 2023). In contrast to numerous studies about redox and productivity conditions, the influence of intensified storm activity on marine conditions during the TOAE lacks detailed assessment to date, although previous studies have identified storm features in many TOAE sections (Hesselbo et al., 2007; Ghadeer and Macquaker, 2011; Trabucho-Alexandre et al., 2012; Suan et al., 2013; Han et al., 2018; Izumi et al., 2018; Xu et al., 2018). Unraveling the relationship between intensified storm activity and marine biogeochemistry during climate warming is also highly relevant for improved assessment of future effects of climate changes on the modern Earth system. In the modern world, burning of fossil fuel and civilization lead to climate warming and warmer sea surface temperatures via release of huge amount of CO_2 into the atmosphere, which increases storm intensity as extreme weather events (e.g., Hansen, 2007; Donnelly et al., 2015).

To better clarify the relation between storminess and marine responses during the TOAE, this study compiles sedimentological, biological and geochemical evidence for storm activity and accompanying marine environmental changes from multiple localities (Fig. 1). The aim of the work is to reveal the relation between storminess and spatial variation of marine properties in TOAE. Our results indicate that, within the framework of local paleogeographic and climatic conditions, intensified storm activity may have acted as an important factor influencing marine primary productivity, nutrient cycling and organic-matter sedimentation during the TOAE.

2. Jurassic climate and storm sedimentation

2.1. Early Jurassic paleogeographic and paleoclimatic conditions

In the Early Jurassic, the supercontinent Pangaea, formed by the assembly of all major continents and plates, consisted of two large landmasses: the Laurasia and the Gondwana continents (Golonka, 2007; Arias, 2008). Nearly equally divided by the Equator, Pangaea was surrounded by the huge Panthalassic Ocean, with the Tethys Ocean wedged into the eastern part of Pangaea. The Karoo and Ferrar Large Igneous Provinces (KFLIP) were associated with breakup of Gondwana during the Early Jurassic (Arias, 2008).

The Early Jurassic was a warm-house world with low or negligible polar ice and high atmospheric CO_2 (Chandler et al., 1992; Landwehrs et al., 2021; Nordt et al., 2022). Further, planetary albedo may have decreased in the Early Jurassic due to limited ice and snow cover and low clouds (Chandler et al., 1992). The symmetric arrangement of landmasses around the warm and tropical Tethys Ocean promoted pronounced monsoonal circulation (megamonsoon) and strong seasonality in Pangaea. Further, based on a broad-scale analysis of variation and distribution of clay minerals and numerical modeling, latitudinal gradients in temperature and precipitation have been recognized, leading to distinct climate belts similar to those of the modern world (Chandler et al., 1992; Dera et al., 2009).

2.2. Intensified storminess during the TOAE

During the TOAE, atmosphere CO_2 concentrations nearly doubled, and paleotemperature proxies from the Boreal and Tethyan realms suggest an increase in sea surface temperatures of 4 to 8 °C (Remírez and Algeo, 2020a; Ruebsam et al., 2020). Although KFLIP emplacement, and consequent CO_2 release, are often suggested to have triggered high atmospheric CO_2, volcanism proxies (i.e., Hg, Hg/TOC) show substantial spatial variation (see Figs. 3, 6, 7, 9,11 below) (Percival et al., 2015). TOAE storminess was proposed to be mainly related to intensified tropical cyclone activity as a consequence of higher atmospheric CO_2 and warmer sea-surface temperatures (Krencker et al., 2015; Yan et al., 2023). Theory and numerical modeling also link strengthened tropical cyclones with higher atmosphere CO_2 levels and sea-surface warming (Emanuel, 1987; Knutson and Tuleya, 2004). Moreover, the enclosed coastline of the western Tethys Ocean and a strong equatorial current driven by paleo-trade winds during TOAE would have favored tropical cyclones (Dera and Donnadieu, 2012; Krencker et al., 2015). As tropical cyclones develop mainly at 5 to 30° N or S of the Equator (Krencker et al., 2015; Han et al., 2018; Yan et al., 2023), TOAE storm activity would have been most prominent in low-latitude regions, consistent with the preservation of thicker and more prominent storm deposits within ~30° of the paleo-Equator, although sedimentological evidence of storm activity is also present at middle paleolatitudes (see below). Similarly, a positive relationship between climate warming and storm activity has been also documented in other periods of Earth history (e.g., Paleocene-Eocene Thermal Maximum, the mid-Pliocene warming event) (Lin et al., 2014; Planas and Paquet, 2016; Giling et al., 2017; Xu et al., 2019; Kiehl et al., 2021; Yan et al., 2016, 2023). In the modern world, increased storminess is associated with sea-surface warming and intensified tropical cyclones, which causes severe property damage and loss of life (Wang and Wu, 2004; Sobel et al., 2016; Kossin et al., 2020). Instrumental observation and theory and numerical simulations suggest human emissions of greenhouse gases, if not prevented, will play an

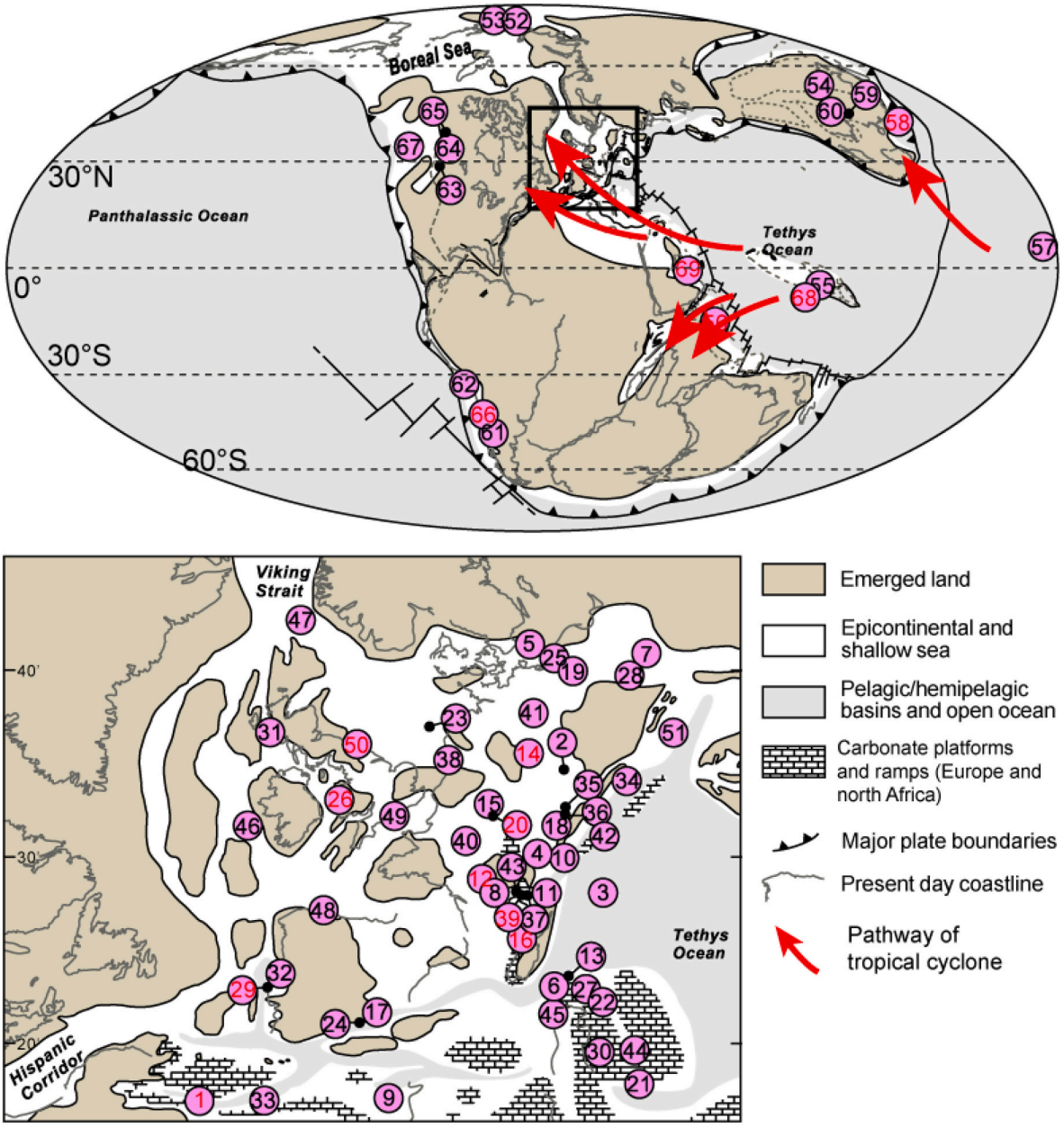

EUROPE AND NORTH AFRICA

1. Amellago
2. Aubach
3. Bachental
4. Belmont
5. Bornholm
6. Breggia
7. Brody-Lubiena
8. Caylus
9. Chaabet El Attaris
10. Creux De L'Ours
11. Cuers
12. Lafarge Quary
13. Dogna
14. Dotternhausen
15. EST433
16. F11-01
17. Fuente La Vidriera
18. Gipf
19. Gorzow Wielkpolski
20. HTM 102
21. Kastelli
22. Kovk
23. L05-04
24. La Cerradura
25. Mechowo
26. Mochras
27. Monte Mangart
28. Parkoszowice
29. Peniche
30. Petousi
31. Raasay
32. Rabacal
33. Ratnek El Kahla
34. R Ka Valley
35. Rietheim
36. Riniken
37. Roqueredonde
38. RWK-01
39. Tournadous
40. Sancerre-Couy
41. Schandelah
42. Skladana Skala
43. Su ges
44. Toka
45. Valdorbia
46. Well 18/25-1
47. Well 34/10-35
48. West Rodiles
49. Winterborne Kingston
50. Yorkshire
51. Zazriva

REST OF THE WORLD

52. Anabar Bay
53. Kelimyar River
54. Anya
55. Bilong Co
56. Nianduo
57. Sakahogi
58. Sakuraguchi-Dani
59. Sichuan Core A
60. Sichuan Core B
61. Arroyo Lapa
62. Asientos
63. Bighorn Creek
64. Core 1-35-62-20W5
65. Core 6-32-75-5W6
66. El Penón
67. Haida Gwaii
68. Sewa
69. Marrat

Fig. 1. Early Toarcian (~183 Ma) paleogeographic map showing previously studied TOAE sections. The sections used in this study are indicated by red numbers inside circles. Modified from Krencker et al. (2015), Remírez and Algeo (2020a), Fu et al. (2021), Alnazghah et al. (2022) and Kemp et al. (2022a). (For interpretation of the references to colour in this figure legend, the reader is referred to the web version of this article.)

important role in further promoting tropical cyclone activity in the future (Sobel et al., 2016; Bhatia et al., 2019). Apart from tropical cyclones, there are also winter and polar cyclones. The winter cyclone is mainly controlled by air mass temperature contrasts (Masselink and Heteren, 2014), and the polar cyclone is developed in the polar marine settings and related to the movement of wind and the transfer of heat in the polar region (Vichi et al., 2019). However, these extratropical cyclones are mainly confined in mid- to high-latitudes

2.3. Types of evidence of storm activity in marine systems

In ancient marine carbonate and siliciclastic successions, storm sedimentation is commonly recorded as event beds with distinctive (bio) stratinomic features (i.e., a "tempestite") (Aigner, 1982; Kreisa and Bambach, 1982; Swift et al., 1987; Brenchley, 1989; Myrow and Southard, 1996). The recognition of storm sedimentation in ancient rocks mainly relies on observation of sedimentary structures and fabrics reflecting rapid hydraulic changes and associated depositional processes during high-energy storm peak and then waning-energy late-storm/post-storm phases (Aigner, 1982; Kreisa and Bambach, 1982; Swift et al., 1987; Brenchley, 1989; Myrow and Southard, 1996). Characteristic sedimentary features of tempestites include: i) a lower part that usually shows normal grading, lags (e.g., shells, pebbles), and erosional bases with sole marks; ii) a middle part that shows a variety of bedforms including parallel lamination, wave-ripple lamination, low-angle cross-stratification, and hummocky cross-stratification (HCS); and iii) an upper part that shows a transition into overlying finer-grained sediment, possibly with primary current lineation or wave ripples (Aigner, 1982; Kreisa and Bambach, 1982; Swift et al., 1987; Brenchley, 1989). Due to spatial variation of storm intensity, sedimentary processes and preservation issues, not all of these features above will be recorded in every tempestite (Brenchley, 1989). Along depositional dip, proximal storm sediments are relatively thick-bedded with coarser grain sizes compared to the background sediment, often forming composite and amalgamated beds. By contrast, distal storm beds are thinner and contain finer grains than proximal storm sediments, with greater mud content (Aigner, 1982).

Sedimentary characteristics observed from modern storm deposits are analogous to those in ancient cases, and commonly include erosional bases, lag deposits, normal grading, and cross-bedding (including HCS) that are indicative of storm activity, as well as a post-storm flood-deposited layer (Kumar and Sanders, 1976; Brackett and Bush, 1986). Factors controlling tempestite occurrence and recognition include the nature of the available sediment, hydrological energy level, storm-generated current direction, distance from shoreline, water depth and degree of post-storm biophysical reworking. These factors are known to affect spatial patterns of modern storm deposits (e.g., Johnson and Belderson, 1969; Nichols, 2009). Laterally, proximal storm deposits in nearshore areas are usually coarser grained and more highly amalgamated than distal, offshore deposits, as that in ancient records (e.g., Aigner, 1982; Myrow and Southard, 1996; Einsele, 2000).

The types of features used to identify storm influence fall into two categories: (1) those that are unambiguously associated with storm processes, and (2) those that may have a storm origin but that can also be produced through other processes (Aigner, 1982; Brenchley, 1989). The most diagnostic feature of storm sedimentation is HCS formed by oscillatory or oscillation-dominated combined flows during storms (Aigner, 1982; Brenchley, 1989; Myrow and Southard, 1996). Also, storm-generated features such as erosional bases, normal grading, and ichnological escape structures are produced through rapid, intermittent sediment deposition. However, some of these features (e.g., basal scouring, normal grading, etc.), while commonly associated with storm processes, can also be generated by turbidites, contourites, and other types of marine currents operating over a wide range of water depths (Tucker and Wright, 1990). An important point is that any single feature, taken in isolation, provides only limited support for storm activity, but the co-occurrence of many characteristic features in the same beds provides significantly stronger support for a storm-related origin. Inferences of a storm origin are reasonable for heterogeneous high-energy deposits exhibiting a mixture of diagnostic and non-diagnostic features of tempestites (Xu et al., 2018).

3. Global survey of storm evidence and related environmental changes in TOAE marine sections

3.1. Survey protocol

Storm sedimentation has been widely reported in TOAE marine settings (Supplementary Table 1). A set of 14 globally distributed TOAE marine sections was evaluated, as they provide evidence of both storm sedimentation and corresponding paleo-environmental conditions. In these 14 sections, data on storminess and marine responses (e.g., primary productivity, redox condition and organic-rich sedimentation) were collected from previous studies (Table 1). The database allows evaluation of the direct link between storminess and marine responses. Otherwise, those TOAE marine sections showing only storminess or marine conditions cause difficulties in the assessment. The 14 sections represent both low-paleolatitude (0 to 30°) sites (Section 3.2; $n = 7$) and mid-paleolatitude (30 to 60°) sites (Section 3.3; $n = 7$), and are from both the Northern and Southern Hemispheres (Table 1). We consider these study sections by paleolatitude (i.e., low- versus mid-latitude) owing to substantial latitude-dependent variation in sedimentary and geochemical characteristics related to storminess. The 14 sections in both low- and mid-paleolatitude areas are from various depositional settings, spanning from marginal marine to basinal settings (Table 1).

3.2. Low-paleolatitude TOAE sites

3.2.1. Lafarge Quarry (France)

The section was deposited in a shallow and marginal setting at a paleolatitude near 30°N in the western Tethys in Early Jurassic (Fig. 1) (Suan et al., 2013). In this section, strata of Toarcian to Bajocian age are fossiliferous and consists of mudstone, marlstone and limestone. The TOAE interval is constrained by ammonite biostratigraphy and characterized by interbedded calcareous beds and laminated clay beds, containing dysoxia-tolerant benthic fauna (Suan et al., 2013).

In the TOAE interval, the calcareous beds are thought to be redeposited by storm and/or storm-related oscillatory currents, based on common sharp and erosive bases, normal grading, low-angle cross bedding, disarticulated fish debris, no preferential orientation of bioclast and bioturbation (Suan et al., 2013). Similar calcareous beds but with a much lower abundance were also found in the distal and basinward settings. The calcareous beds were deposited around the peak of TOAE NCIE (Suan et al., 2013).

Compared to the laminated clay beds ($CaCO_3$: 26 to 43 wt%; TOC: 2.4 to 9.6 wt%), the calcareous beds interpreted as storm deposits show high $CaCO_3$ content (80 to 93 wt%) and low TOC (0.14 to 1 wt%) (Fig. 2). Moreover, TOC and HI values overall increase across the TOAE interval coeval with negative $\delta^{13}C_{carb}$ and $\delta^{13}C_{org}$ excursions (Suan et al., 2013; Charbonnier et al., 2020) (Fig. 2). In the TOAE interval, thin lamination and lack of bioturbation suggest oxygen depletion in the laminated clay beds, while the calcareous beds related to storminess reflect more oxic conditions (Suan et al., 2013).

3.2.2. Tournadous section (France)

During the late Pliensbachian-early Toarcian, the Causses Basin (paleolatitude between 25 and 30°N) was a small and intracratonic basin within the European epicontinental sea (Mailliot et al., 2009). In the Tournadous section within the basin, the upper Pliensbachian Marnes de Villeneuve Formation consists of marls and limestones with frequent bioturbation, while the overlying lower Toarcian Schistes Carton facies displays laminated shales at the base (Mailliot et al., 2009).

Table 1
Sedimentary and geochemical information of TOAE marine sections in this study.

Section	Depositional setting	Paleo-latitude and -hemisphere	Storm-related bed thickness	Storm-related sedimentary structures	TOAE marine property	Key references
Lafarge Quarry, France	Epicontinental marine margin, restricted, western Tethys	Low latitude (near 30°N), Northern Hemisphere	Thin bedded	Low-angle cross bedding, sharp and erosive bases, normally graded lamination and bioturbation	No persistent ocean anoxia; water stratification; organic-rich sedimentation	Suan et al., 2013; Charbonnier et al., 2020
Tournadous, France	Epicontinental basin, restricted, western Tethys	Low latitude (between 25 and 30°N), Northern Hemisphere	Thin bedded	Enhanced influx of plant debris and coarser siliciclastic grains with HCS	Ocean anoxia, interrupted by brief seafloor oxygenation events; black shale	Mattioli and Pittet, 2004 Mailliot et al., 2009
Peniche,Portugal	Hemipelagic setting connected with open ocean, western Tethys	Low latitude (near 23°N), Northern Hemisphere	Thicker bedded	Enhanced influx of coarser siliciclastic grains, sharp bases, normal grading, load structures, convolute bedding, HCS	Mainly oxic settings; low TOC	Duarte, 1997; Kullberg et al., 2001; Pittet et al., 2014; Hesselbo et al., 2007; Hermoso et al., 2009; Correia et al., 2017; Fantasia et al., 2019
Amellago, Morocco	Open marine, western Tethys	Low latitude (between 17 and 20°N), Northern Hemisphere	Thicker bedded	HCS, the depauperate fauna, the complete loss of lithiotid-rich facies and very common occurrence of plant debris	Mainly oxic setting; low TOC	Krencker et al., 2015, 2020; Bodin et al., 2016; Boulila et al., 2019
Sewa, China	Open marine, eastern Tethys	Low latitude (0–10°S), Northern Hemisphere	Thicker bedded	Enhanced terrestrial influx of coarser siliciclastics	Mainly oxic; low TOC	Fu et al., 2021
Marrat, Saudi Arabia	Open marine, eastern Tethys	Low latitude (0–10°S), Southern Hemisphere	Thicker bedded	Enhanced influx of siliciclastic grains, HCS, parallel lamination, climbing and combined-flow ripples	Oxic marine settings; low TOC	Al-Hussaini et al., 2021; Alnazghah et al., 2022
Nianduo, China	Open marine, eastern Tethys	Low latitude (21–26°S), Southern Hemisphere	Thicker bedded	HCS, erosional bases, graded bedding, parallel laimation, gutter casts and climbing ripples	Mainly oxic-suboxic marine conditions; low TOC	Han et al., 2016, 2018, Han et al., 2022a, 2022b; Jiang et al., 2020
Yorkshire coast, UK	Epicontinental basin, restricted, western Tethys	Mid-latitude (35–40°N), Northern Hemisphere	Thin bedded	Erosional base, normally graded bedding, gutter casts	Enhanced water stratification, anoxic to euxinic conditions, interrupted by brief seafloor oxygenation events; black shale	Wignall et al., 2005; Pearce et al., 2008; Nielsen et al., 2011; Ghadeer and Macquaker, 2011; Salem, 2013; French et al., 2014; Baroni et al., 2018
Mochras Borehole, UK	Epicontinental basin, restricted, western Tethys	Mid-latitude(near 35°N), Northern Hemisphere	Thin bedded	Enhanced influx of coarser siliciclastic grains and plant debris, faint lamination, ripples and flame structure	No persistent ocean anoxia; water stratification, but transient photic-zone euxinia; increased TOC but no black shale	Jenkyns et al., 2001; Percival et al., 2015, 2016; Xu et al., 2018
Core F11–01, Netherlands	Epicontinental basin, western Tethys	Mid-latitude (35–40°N), Northern Hemisphere	Thin bedded	Erosional bases, cross lamination, normally graded bedding, scour-and-fill structures and bioturbation	Extension of anoxic conditions up to sediment-water interface, while the overlying bottom water was prevailingly oxic; black shale	Trabucho-Alexandre et al., 2012
Core HTM 102, France	Epicontinental basin, restricted, western Tethys	Mid-latitude (35–40°N), Northern Hemisphere	Thin bedded	Erosional base, graded bedding, low angle cross lamination, chaotic and winnowed fossil accumulation	Intermittent water column anoxia (even euxinia) in the T-OAE interval, interrupted by water-mixing events; black shale	van Breugel et al., 2006
Dotternhausen, Germany	Epicontinental basin, restricted, western Tethys	Mid-latitude (30–35°N), Northern Hemisphere	Thin bedded	Enhanced influx of coarser siliciclastic grains with sharp bases	Ocean anoxia, interrupted by brief seafloor oxygenation events; black shale	Röhl et al., 2001; Dickson et al., 2017; Them et al., 2018; Wang et al., 2021
Sakuraguchi-dani, Japan	Open marine margin, Panthalassic Ocean	Mid-latitude(ca. 35–40°N), Northern Hemisphere	Thicker bedded	Enhanced terrestrial influx and sudden occurrence of sandstone beds. The sandstone beds show increase in grain size, floated mud clasts, cross-lamination and higher degree of bioturbation	Mainly oxic settings; low TOC	Kemp and Izumi, 2014; Izumi et al., 2018; Kemp et al., 2019; Chen et al., 2023
El Penõn, Chile	open marine setting, eastern Tethys	Mid-latitude (30–40°S), Southern Hemisphere	Thicker bedded	Erosive bases, accumulation of poorly sorted, broken shells, and elevated siliciclastic influx	Mainly oxic marine settings, low TOC	Fantasia et al., 2018a, 2018b

The TOAE interval is defined by ammonite and calcareous nannofossil biostratigraphy and is marked by a negative $\delta^{13}C_{carb}$ excursion recorded in the lower Toarcian Schistes Carton (Fig. 2) (Mailliot et al., 2009).

Within the lower Schistes Carton, some siliciclastic beds are enriched in fish remains and silty materials with HCS. Tempestites with HCS are common, generally amalgamated, and can reach meter-scale thickness in shallow-water areas (Mattioli and Pittet, 2004). The storm beds correlate with the Toarcian NCIE and water-column oxygenation events

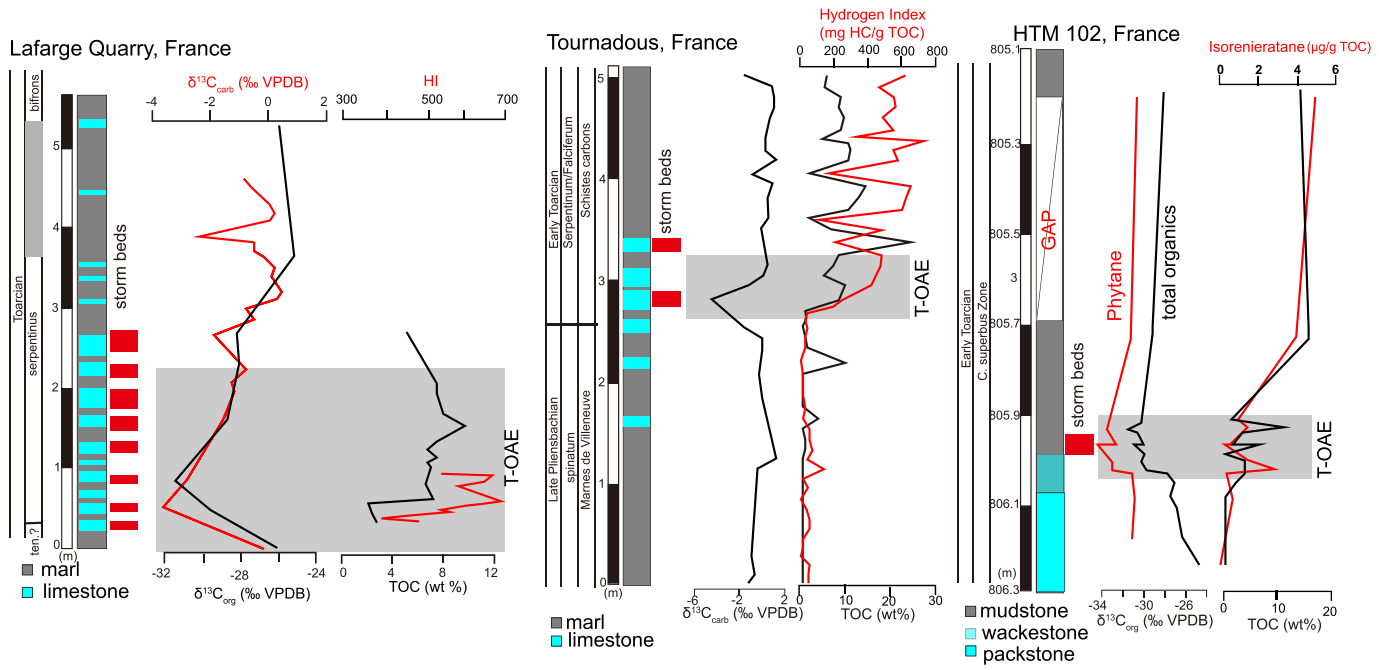

Fig. 2. Lithological and geochemical data from Lafarge Quarry (France, number 12 in Fig. 1), Tournadous (France, number 39 in Fig. 1) and HTM 102 Boreholes (France, number 20 in Fig. 1). The TOAE interval is indicated by the grey fields. Storm-related deposits often occur as thin (cm to dm scale) beds and shows common sharp and erosive bases, normal grading, bioturbation and scarce HCS. Sources: (1) Lafarge Quarry, Suan et al. (2013) and Charbonnier et al. (2020); (2) F11–01, Mailliot et al. (2009); (3) HTM 102, van Breugel et al. (2006).

(Mailliot et al., 2009).

The TOAE interval overall shows increased TOC (8% on average) dominated by marine organic matter with higher HI ratios (>400 mg HC/g TOC on average) than the pre-TOAE interval (Fig. 2). Moreover, decreased $CaCO_3$ contents co-occur with greatly reduced calcareous fossil abundance, including both nannofossils and foraminifera (Mailliot et al., 2009). Sedimentological, paleontological (i.e., calcareous nannofossils and foraminifera) and mineralogical (pyrite) analyses indicate alternating oxidizing (siliciclastic-rich beds) and hypoxic-anoxic (organic-rich beds) conditions during the TOAE (Mailliot et al., 2009).

3.2.3. *Peniche (Portugal)*

During late Pliensbachian-early Toarcian, the Peniche section in the Lusitanian Basin (paleolatitude of ca. 23°N) was deposited in a hemipelagic setting connected with the open western Tethys Ocean (Hesselbo et al., 2007; Hermoso et al., 2009; Correia et al., 2017; Fantasia et al., 2019). In this section, the Lemede Formation of latest Pliensbachian (*spinatum* Zone) to earliest Toarcian age (*polymorphum* Zone ≈ *tenuicostatum* Zone in the Boreal realm) consists of fossiliferous and interbedded limestones and marls. The overlying Cabo Carvoeiro Formation of the upper *polymorphum* and *levisoni* zones (≈*serpentinum* Zone in the Boreal realm) consists of sandy limestones and marls that are sparsely fossiliferous. In the Cabo Carvoeiro Formation, the TOAE interval is defined based on biostratigraphy and NCIEs (−4‰ to −3‰ for $\delta^{13}C_{carb}$; to −7‰ for $\delta^{13}C_{org}$) (Hesselbo et al., 2007) (Fig. 3).

During the most negative part of TOAE NCIE, turbiditic, siliciclastic sediments inferred to have been triggered by storm activity are common (Hesselbo et al., 2007), while biogenic carbonate production collapsed. The siliciclastic beds (sandstone) vary in thickness (usually <75 cm), and show erosional bases, normal grading and sometimes, load structures and convolute bedding. Associated with the siliciclastic influx were more abundant ooids. Parallel lamination, symmetrical ripples, and HCS are locally present (Duarte, 1997; Kullberg et al., 2001; Pittet et al., 2014).

Within the TOAE interval, TOC is relatively low (~0.5–0.6 wt%) and dominated by terrestrial organic matter, as evidenced by high oxygen index (OI) and low HI values and palynological analysis (Correia et al., 2017; Fantasia et al., 2019) (Fig. 3). The marine organic fraction witnessed a reduction of dinoflagellate algae (i.e., a plankton crisis) and a rise of prasinophyte algae in the TOAE (Correia et al., 2017). Detrital index and Ca isotope data suggest enhanced continental chemical weathering and possible ocean acidification in the lower TOAE (Brazier et al., 2015; Fantasia et al., 2019). However, B isotope data imply an overall reduced seawater pH from the Pliensbachian-Toarcian boundary to the TOAE, and increased ocean pH at the base of TOAE (Müller et al., 2020) (Fig. 3). A paleotemperature record based on brachiopod oxygen isotopes suggests strong warming during the early TOAE (Suan et al., 2008). While higher P_{tot} contents occur in the lower TOAE, mainly oxic-suboxic conditions are indicated by redox-sensitive elements (enriched in Mn but not Mo, V and Ni) (Fantasia et al., 2019), higher Tl isotope values (Nielsen et al., 2011), and lower Mo isotope values (Dickson et al., 2017) (Fig. 3). Additionally, the TOAE interval shows Hg and Hg/TOC spikes (Fantasia et al., 2019).

3.2.4. *Amellago (Morocco)*

In the Dades Valley of Central High Atlas Basin, the upper Pliensbachian to uppermost middle Toarcian succession (paleolatitude of 17 to 20°N) is well studied, including the Ouchbis Formation, Tagoudite Formation and Tafraout Formation (Krencker et al., 2015, 2020; Bodin et al., 2016; Boulila et al., 2019). The Ouchbis Formation mainly consists of mudstone to packstone, while the overlying Tagoudite Formation contains abundant clay-, silt- and sandstones. The Tafraout Formation is characterized by ooid-rich limestones. Constrained by biostratigraphy (e.g., ammonite and calcareous nannofossils) and chemostratigraphy (e.g., carbon isotope), the Pliensbachian-Toarcian transition shows a major lithological change from carbonate-rich to siliciclastic and ooid-rich rocks (Krencker et al., 2015, 2020; Bodin et al., 2016; Boulila et al., 2019).

The common occurrence of storm deposits was associated with increased terrestrial fluxes in the TOAE interval, and is characterized by HCS, depauperate fauna, complete loss of lithiotid-rich facies and the very common occurrence of plant debris (Krencker et al., 2020). The

HCS can be amalgamated or isolated and separated by clay intervals. Wavy cross-bedding, oysters and brachiopods are also observed, despite a low faunal abundance (Krencker et al., 2020).

In this shallow-marine section, the neritic carbonate factory showed a change from biogenic-dominated (with diverse bioclasts) to chemical/microbial-dominated production with abundant ooids associated with NCIEs (−5‰ to −2‰ for $\delta^{13}C_{carb}$; to −4‰ for $\delta^{13}C_{org}$) and enhanced siliciclastic input (Fig. 4). Palynological analysis shows a reduction of nannofossils during the TOAE, and the organic matter is dominated by terrestrial organic matter. Increased P_{tot} contents related to continental fluxes developed during the TOAE (Bodin et al., 2010, 2016) (Fig. 4). There was a lack of organic-rich sedimentation (TOC <0.5% at average), TOC decrease and no persistent oceanic anoxia during the TOAE.

3.2.5. Sewa (China)

During the TOAE interval, the Sewa section in the Qiangtang Basin (paleolatitude of 0 to 10°S) represents a shelf, open-marine setting in eastern Tethys (Fu et al., 2021). Based on ammonite biostratigraphy, spores and pollen grains, the Lower Jurassic Quse Formation consists of mainly shallow marine mudstone, calcareous mudstone, silty mudstone and marl, with sedimentary structures such as horizontal and convolute bedding (Fu et al., 2021).

Coarse-grained siliciclastics of terrigenous origin are interbedded with the marine mudstone deposits, correlating with the most negative interval of the TOAE NCIE (Fu et al., 2021). The enhanced influx of coarse-grained siliciclastics coincided stratigraphically with similar lithologies in geologically widespread marine basins, which were attributed to a climatic control (increase runoff and/or storm activity) (Fu et al., 2021).

Different from a more proximal section in the Qiangtang Basin showing organic-rich shale sedimentation in the restricted lagoonal setting, the TOAE interval in the Sewa section is characterized by organic-poor (ca. 0.5 wt%) sediment and a NCIE (−4‰ to −3‰ for $\delta^{13}C_{carb}$) (Fig. 4). Redox-sensitive elements and low TOC/P suggest long-term oxidation in the TOAE (Fu et al., 2021) (Fig. 4).

3.2.6. Marrat (Saudi Arabia)

On the northeastern margin of the Arabian Plate, the Marrat Formation represents open-marine shelf deposition (paleolatitude of 0 to 10°S) during the TOAE, as dated by ammonite biostratigraphy (Al-Hussaini et al., 2021; Alnazghah et al., 2022). The Marrat Formation can be divided into three lithological units: a transition from siliciclastic to carbonate deposits in the lower Marrat; reddish mudstones (claystone) with intercalations of sandstone and siltstone in the middle Marrat; and mainly carbonates and anhydrites in the upper Marrat (Fig. 5) (Al-Hussaini et al., 2021). In the middle Marrat, a NCIE (ca. –5‰ for $\delta^{13}C_{org}$) marks the TOAE (Fig. 5).

Compared with the lower and upper Marrat, the middle Marrat records an enhanced influx of coarse-grained siliciclastic sediment including silt and sand, and a near-absence of macrofauna during the TOAE NCIE. In the sandy sediment, HCS and swaley cross-stratification are observed with parallel lamination, climbing and combined-flow ripples, suggesting high-energy and rapid sedimentation related to storm activity (Al-Hussaini et al., 2021).

In the TOAE interval, increased terrestrial input with higher chemical index of alteration values suggests elevated continental weathering intensity (Al-Hussaini et al., 2021). However, the TOC is low (0.3 to 0.9 wt%). Elemental proxies (e.g., Cr, U, V, Ba, Cu, Ni) and the reddish colour of sediment indicate oxic conditions and low primary productivity, which may have been related to terrestrial fluxes and the high-energy depositional setting (Alnazghah et al., 2022) (Fig. 5).

3.2.7. Nianduo (China)

During the Early Jurassic, the Nianduo section was located in the marine realm of southeastern Tethys Ocean with a paleolatitude of 21 to 26°S (Han et al., 2018, 2022a, 2022b). The upper Pliensbachian to lower

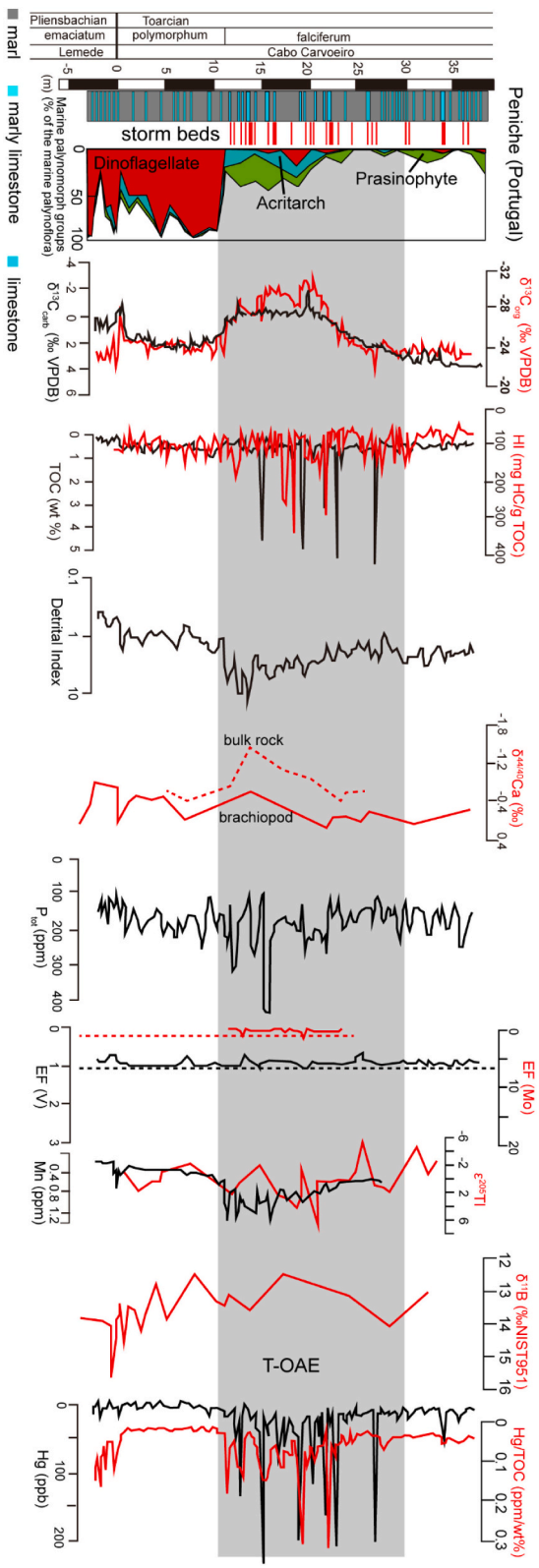

Fig. 3. Lithological, biological and geochemical data from Peniche (Portugal, number 29 in Fig. 1). The TOAE interval is indicated by the grey field. Storm-related deposits (dm to m scale) show increased siliciclastic influx with erosive bases. Sources: lithology and storm sedimentation, Hesselbo et al. (2007) and Fantasia et al. (2019); palynology, Correia et al. (2017); carbon isotope, TOC, HI, detrital index, Mo, V, Mn, Hg and Hg/TOC, Fantasia et al. (2019); Ca isotope, Brazier et al. (2015); Tl isotope, Nielsen et al. (2011); B isotope (Müller et al., 2020).

Toarcian beds consist mainly of carbonate rocks assigned to the Pupuga and Nieniexiongla formations (Fig. 5). The Pupuga Formation consists of bioclastic limestone representing shallow marine carbonate platform settings, while the overlying Nieniexiongla Formation mainly consists of micritic limestone implying a deeper, middle to outer ramp setting (Han et al., 2018, 2022a, 2022b).

The sediment of middle to outer ramp in the Nieniexiongla Formation was frequently interrupted by storm activity that deposited coarse-grained oolitic and siliciclastic clasts (Han et al., 2018). This storm-related sediment is mainly found in the lower and upper Nieniexiongla Formation, and is characterized by hummocky and swaley cross stratification, sharp erosive bases, graded bedding, parallel lamination, U- or V-shaped gutter casts, and climbing ripples (Han et al., 2016, 2018).

Defined by ammonite and foraminiferal biostratigraphy, the TOAE interval shows a NCIE (ca. –2.5‰ for $\delta^{13}C_{org}$), which is coeval with the occurrence of abundant tempestites, enhanced terrestrial fluxes, and extinction of benthic foraminifera (Han et al., 2018, 2022a, 2022b; Jiang et al., 2020). The combination of common bioturbation, stronger storm activity and low TOC (0.05 to 0.3 wt%) argue against persistent oceanic anoxia, while higher Mn and lower Ce/Ce* suggest possibly suboxic conditions due to ocean deoxygenation (Fig. 5).

3.3. *Mid-paleolatitude TOAE sites*

3.3.1. *Yorkshire coast (UK)*

The Hawsker Bottoms section on the Yorkshire coast was deposited at a mid-paleolatitude (between 35 and 40°N) epicontinental marine setting in a restricted basin during the late Pliensbachian and early Toarcian (Fig. 1) (Wignall et al., 2005; Salem, 2013; Remírez and Algeo, 2020b). Based on biostratigraphy and sedimentology, the Grey Shale Member (*tenuicostatum* Zone) and overlying Mulgrave Shale Member (*falciferum* Zone) record a marine transgressive sequence of early Toarcian age (Wignall et al., 2005; Salem, 2013). In the Mulgrave Shale, the TOAE interval is characterized by organic-rich mudstone (TOC of up to 14%) and a NCIE (Wignall et al., 2005; McArthur et al., 2008; Salem, 2013) (Fig. 6).

Immediately below and at the base of the TOAE interval, increased terrestrial input deposited mudstone containing more silty and sandy grains. In these coarser-grain mudstone layers (5 to 40 mm in thickness), there are storm-generated sedimentary structures (e.g., erosional base, normal grading, wave-enhanced sediment gravity flows and gutter casts) (Ghadeer and Macquaker, 2011; Salem, 2013). The storm-generated sediment corresponds to brief seafloor oxygenation events (indicated by bioturbation and bivalve colonization) (Wignall et al., 2005; Ghadeer and Macquaker, 2011; Salem, 2013).

Palynological and organic geochemical analyses show that the organic matter is mainly of marine origin with high hydrogen index (HI) values and increases across the TOAE. During the TOAE, marine primary producers experienced a algae bloom with change from dinoflagellates to sphaeromorphs (Salem, 2013; French et al., 2014; Slater et al., 2019). Enhanced continental chemical weathering is supported by increased Sr and Os isotope values that were greatest at the base of the TOAE but then decreased upwards (Cohen et al., 2004). In combination with high TOC, a positive excursion of nitrogen isotopes ($\delta^{15}N_{bulk}$) during the TOAE (Fig. 6) was proposed to reflect increased marine primary productivity (Jenkyns et al., 2001). On the other hand, multiple sedimentological (e.g., fine lamination), biological (e.g., biomarker), mineralogical (e.g., degree of pyrite) and geochemical (e.g., Mo, S and Tl isotopes, TOC/P) suggest enhanced water-column stratification and anoxic to euxinic basinal settings during the TOAE (Pearce et al., 2008; Nielsen et al., 2011; French et al., 2014; Baroni et al., 2018) (Fig. 6). Despite higher Hg content across the TOAE, Hg/TOC ratios decrease, possibly reflecting a terrestrial (rather than volcanic) Hg source (Percival et al., 2015).

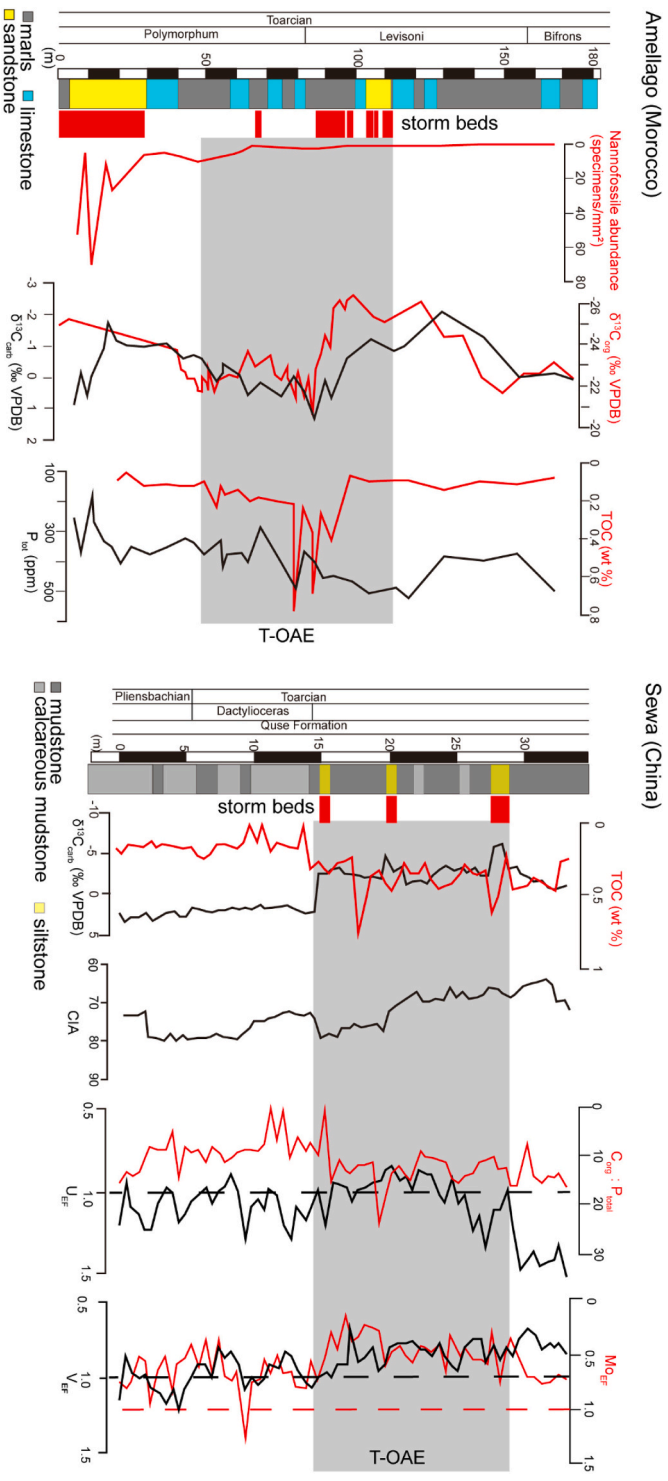

Fig. 4. Lithological and geochemical data from Amellago (Morocco, number 1 in Fig. 1) and Sewa (China, number 68 in Fig. 1). The TOAE interval is indicated by the grey field. Storm-related deposits (dm to m scale) are common and ubiquitous in the TOAE interval, and are characterized by hummocky cross-stratification, depauperate fauna, the complete loss of lithiotid-rich facies and increased terrestrial fluxes. Sources: (1) Amellago, lithology and storm deposit data, Bodin et al. (2016), Krencker et al. (2015); palynology, TOC and P, Bodin et al. (2010, 2016). (2) Sewa, from Fu et al. (2021).

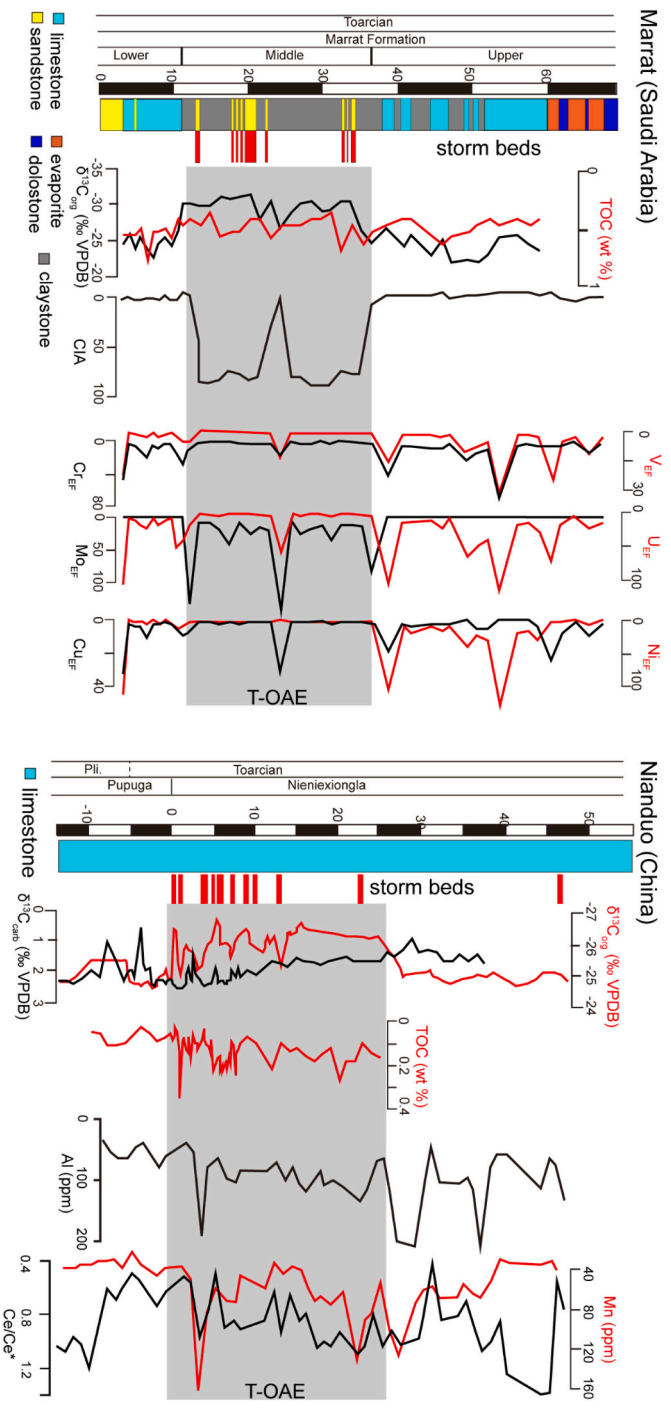

Fig. 5. Lithological and geochemical data of Marrat (Saudi Arabia, number 69 in Fig. 1) and Nianduo (China, number 56 in Fig. 1). The TOAE interval is indicated by the grey field. Storm activity caused thicker (dm to m scale) bedded gravity-flow deposits showing erosive base, poorly sorted, broken shells, and increased terrestrial debris. Sources: (1) Marrat: Alnazghah et al. (2022); (2) Nianduo: Han et al. (2018, 2022a, 2022b).

3.3.2. *Mochras Borehole (UK)*

The Mochras Farm Borehole section is within the Cardigan Bay Basin, which was located in the mid-paleolatitude (near 35°N) European epicontinental seaway during the Early Jurassic (Fig. 1) (Xu et al., 2018). In the borehole, a thick succession of Lower Jurassic strata consists of mudstone, marl and muddy limestone deposited in an open-marine and basinal setting (Sellwood and Jenkyns, 1975; Xu et al., 2018). Constrained by ammonite and foraminifera biostratigraphy, the Pliensbachian-Toarcian succession commonly contains plant debris and siliciclastic silt and sand (Cope, 1984).

In the TOAE, storm-related quartzose siltstone layers (1 to 10 cm thick) occur with coarser grains within mudstones. The thin siltstone beds are discrete, and some beds show faint lamination, ripples, flame structures, and/or abundant cm-scale woody fragments. These coarser-grained siltstone layers correspond to the nadir of the NCIE and coincided with deposition of similar lithologies elsewhere in shallow- or deep-marine settings (Xu et al., 2018).

The TOAE interval is characterized by: i) NCIEs of both $\delta^{13}C_{carb}$ and $\delta^{13}C_{org}$; ii) increased TOC contents (up to 2.5%); and iii) a lack of black shale beds (Jenkyns et al., 2001; Xu et al., 2018) (Fig. 7). During the TOAE, increased $^{187}Os/^{188}Os$ values reflect enhanced continental chemical weathering fluxes and an intensified hydrological cycle (Percival et al., 2016; Xu et al., 2018) (Fig. 7). Moreover, a positive $\delta^{15}N_{tot}$ excursion at the TOAE was proposed to imply increased primary productivity (Jenkyns et al., 2001), and biomarkers (e.g., C_{30}-sterane/$C_{(27+28+29+30)}$-steranes, gammacerane/C_{30}-hopane) suggest more algal components in marine primary producers (Xu et al., 2018). Common bioturbation and a lack of distinct black shale deposition throughout the TOAE sediment disapprove persistent oceanic anoxia and water-column stratification, whereas transient photic-zone euxinia is indicated by trace amounts of gammacerane and isorenieratane (Xu et al., 2018). Higher siderite abundance was thought to be related to early diagenetic organic matter decomposition and low ocean sulfate content (Xu et al., 2018) (Fig. 7). Increased Hg/TOC suggests a possibly increased flux of volcanic or terrestrial Hg during the TOAE (Percival et al., 2015).

3.3.3. *Core F11–01 (The Netherlands)*

In the Core F11–01 of Dutch Graben, the Posidonia Shale Formation represents Toarcian (*tenuicostatum* to *falciferum* zones) sedimentation in a restricted basinal setting at 35–40°N paleolatitude (Fig. 1) (Trabucho-Alexandre et al., 2012). A negative $\delta^{13}C_{org}$ excursion characterizes the TOAE interval with increased TOC content (up to 16%). The organic matter contains both marine algae and terrestrial material (Fig. 8) (Trabucho-Alexandre et al., 2012).

In the Posidonia Shale Formation, the shales are dominated by a stacked succession of thin (< 10 mm) beds. In these thin beds, detailed sedimentological analyses reveal common erosional bases, cross-bedding, normal grading, scour-and-fill structures and bioturbation, reflecting frequent interruption by high-energy and oxygenation events (possibly related to storms) and no persistent watermass anoxia (Trabucho-Alexandre et al., 2012). Moreover, these thin beds are concentrated in the most negative interval of TOAE NCIE. Interestingly, short-term high-energy and oxygenation events related to storminess observed in thin sections were not geochemically detected by redox-sensitive elements (Trabucho-Alexandre et al., 2012).

During the TOAE, terrestrial flux indicators (e.g., Al and Ti) and nutrient elements (e.g., Ba, P) decrease upwards. On the other hand, the TOAE interval is enriched in redox-sensitive elements including Mo and V, but not Mn and Fe (Fig. 8). The enrichment of Mo and V, as well as abundant euhedral and diagenetic pyrites, was suggested to form due to extension of anoxic conditions in bottom water (Trabucho-Alexandre et al., 2012).

3.3.4. *Core HTM 102 (France)*

Core HTM 102 was drilled in the Paris Basin, which was part of a shallow northern epicontinental sea (Boreal Realm; 35 to 40°N) in early Toarcian (van Breugel et al., 2006). In the core, the TOAE interval is constrained biostratigraphically by nannofossils, and is characterized by a negative $\delta^{13}C_{org}$ excursion (ca. –6.5‰) (Fig. 2). TOC increases across the TOAE from 0.5 wt% to 1–10 wt% (Fig. 2) (van Breugel et al., 2006).

A tempestite interval at the lower part of the TOAE is characterized by erosional bases, chaotic and winnowed fossil accumulation, normal grading, and low-angle cross-bedding. Moreover, the tempestite interval records benthic colonization and bioturbation, and corresponds with the

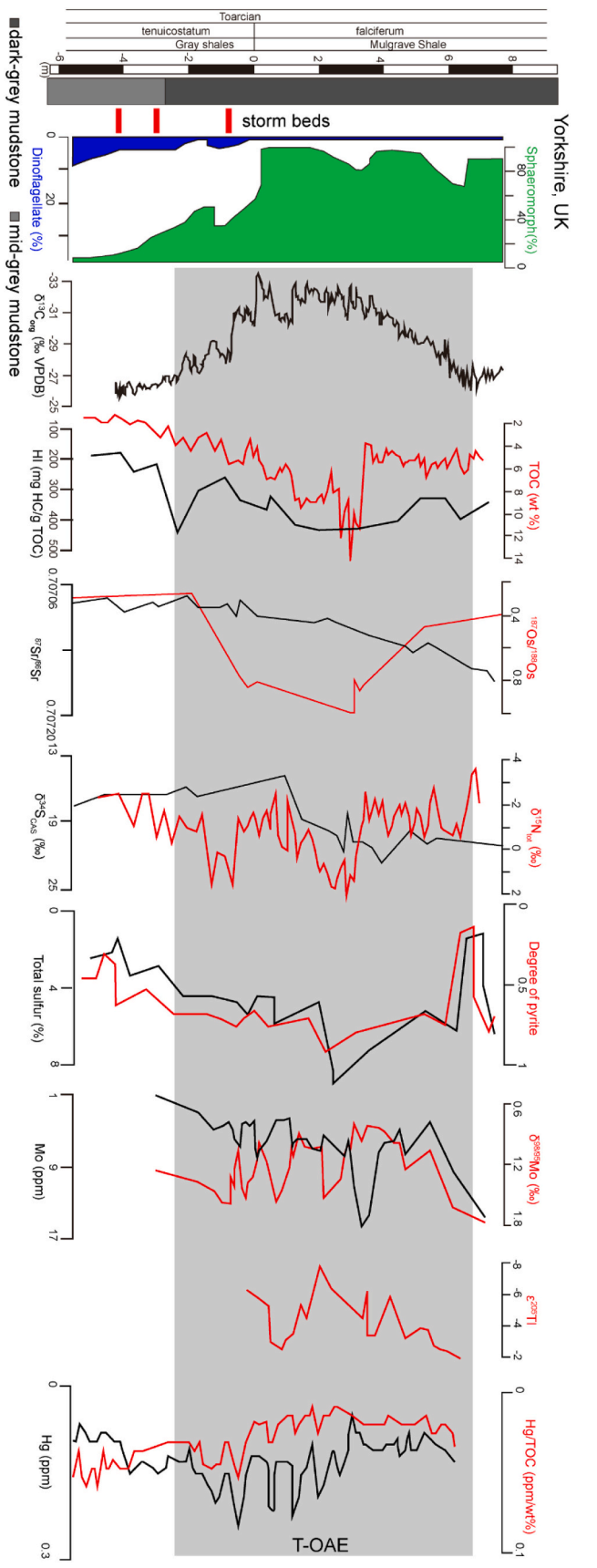

(caption on next column)

Fig. 6. Lithological, biological and geochemical data of the Hawsker Bottoms section in Yorkshire (UK, number 50 in Fig. 1). The TOAE interval is indicated by the grey field. Putative storm deposits occur as thin (cm to dm scale) beds showing sedimentary structures like HCS, basal scouring, and normal grading, associated with brief seafloor oxygenation events (indicated by bioturbation and bivalve colonization) immediately below and at the base of the TOAE interval. Sources: lithology and storm sedimentation, Wignall et al. (2005), Ghadeer and Macquaker (2011) and Salem (2013); palynology, Slater et al. (2019); carbon isotope, TOC and HI, Jenkyns et al. (2001), McArthur et al. (2008), Salem (2013), and French et al. (2014); Sr and Os isotope, McArthur et al. (2008), Cohen et al. (2004); S isotope, Newton et al. (2011); N isotope, Jenkyns et al. (2001); Tl isotope, Nielsen et al. (2011); total sulfur, Mo and Mo isotope, McArthur et al. (2008); Hg and Hg/TOC, Percival et al. (2015).

lowest $\delta^{13}C_{org}$ values (van Breugel et al., 2006).

Sedimentological and biomarker (e.g., pristane, phytane, n-alkanes, isorenieratane) analyses suggest a change from well-mixed water column with intermittent euxinia to long-term stagnant and anoxic water column interrupted by short-term oxygenation during the TOAE interval (van Breugel et al., 2006). Further, the water column anoxia extended into the photic zone (van Breugel et al., 2006).

3.3.5. *Dotternhausen (Germany)*

The Dotternhausen section represents shallow marine deposition in a semi-restricted basin (ca. 30 to 35°N) in the European epeiric sea, wherein the lower Toarcian succession (Posidonia Shale) consists mainly of marls and marly clays interbedded with a few nodular limestone beds (Röhl et al., 2001). Based on biostratigraphy and chemostratigraphy, the TOAE interval displays a negative $\delta^{13}C_{org}$ excursion (−7‰ to −5‰) (Fig. 9). During the TOAE, a change was observed from highly bioturbated light grey marls to well laminated black shales.

Storm sedimentation is recorded at Dotternhausen as thin (< 1 mm) silty layers with sharp bases within laminated shales (Röhl et al., 2001; Dickson et al., 2017; Them et al., 2018; Wang et al., 2021). The storm sedimentation led to the occurrence of a low diversity but occasionally highly abundant benthic fauna in a few horizons, and corresponds to most negative part of TOAE NCIE (Fig. 9) (Röhl et al., 2001; Dickson et al., 2017).

During the TOAE, increased TOC (up to 20–30%) is dominated by marine organic matter (Wang et al., 2020, 2021) (Fig. 9). A nearby location 2 km away (Dormettigen) shows a transition from terrestrial to marine organic matter across from pre-TOAE to the TOAE, with the TOAE marine organic matter showing a replacement of dinoflagellates by prasinophyte algae and *Spheripollenites* (Ajuaba et al., 2022). Low $\delta^{15}N_{tot}$ values (+0.3‰ to +2.5‰) with no obvious variation suggest enhanced nitrogen fixation by cyanobacteria during the TOAE (Wang et al., 2021). Well-laminated black shales containing framboidal pyrites and geochemical proxies (e.g., redox-sensitive elements including Mo, U, V and Mn, Mo isotope, Fe species, Tl isotope) support Toarcian oceanic anoxia (Fig. 9). The oceanic anoxia was occasionally interrupted by transient oxygenation events related to distal storm sedimentation (Röhl et al., 2001; Dickson et al., 2017; Them et al., 2018; Wang et al., 2021). No clear enrichment of Hg and Hg/TOC were observed during the TOAE (Them et al., 2019) (Fig. 9).

3.3.6. *Sakuraguchi-dani (Japan)*

In the early Jurassic, the Sakuraguchi-dani section was deposited on a shallow shelf along a tectonically active continental margin (ca. 35 to 40°N) of the Panthalassic Ocean (Kemp and Izumi, 2014; Kemp et al., 2019; Chen et al., 2023). The Pliensbachian-Toarcian succession (Nishinakayama Formation) consists of shallow marine silty shale, mudstone and fine-grained sandstone. Constrained by carbon-isotope chemostratigraphy and ammonite biostratigraphy, the TOAE interval occurs in the Nb member (predominantly dark silty shale but with intercalated fine-grained sandstone and laminated shales) of the Nishinakayama Formation.

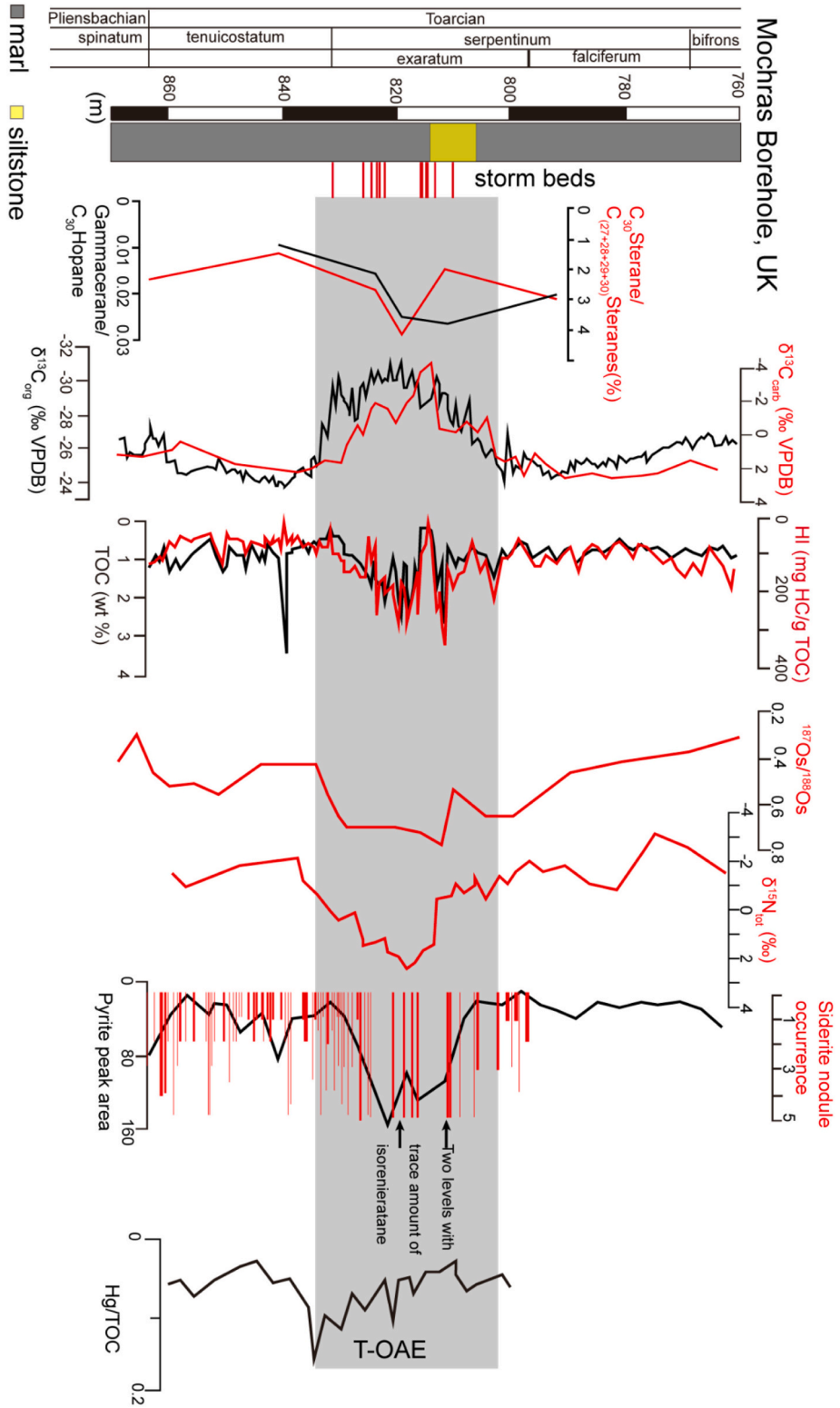

Fig. 7. Lithological, biological and geochemical data of the Mochras Farm Borehole section (UK, number 26 in Fig. 1). The TOAE interval is indicated by the grey field. Storm activity caused thin (cm to dm scale) bedded gravity flow deposits with coarse grains. Sources: lithology and storm sedimentation, Sellwood and Jenkyns (1975), Xu et al. (2018) and Ullmann et al. (2022); biomarker, carbon isotope, TOC and HI, Xu et al. (2018); Os isotope, Percival et al. (2016); N isotope, Jenkyns et al. (2001); Siderite nodule occurrence and pyrite peak area, Xu et al. (2018); Hg/TOC, Percival et al. (2015).

Enhanced terrestrial fluxes are suggested by the sudden appearance of siltstone and sandstone beds during the TOAE (Kemp et al., 2019). In the silty beds, there are sharp bed contacts and a gradual, consistent fining-upward motif, which resemble wave-enhanced sediment gravity flow beds or tempestites (Izumi et al., 2018). The sandstone beds contain a suite of features including floating mud clasts, cross-bedding, and bioturbation, that are consistent with storm/hyperpycnal flow deposition (Izumi et al., 2018; Kemp et al., 2019).

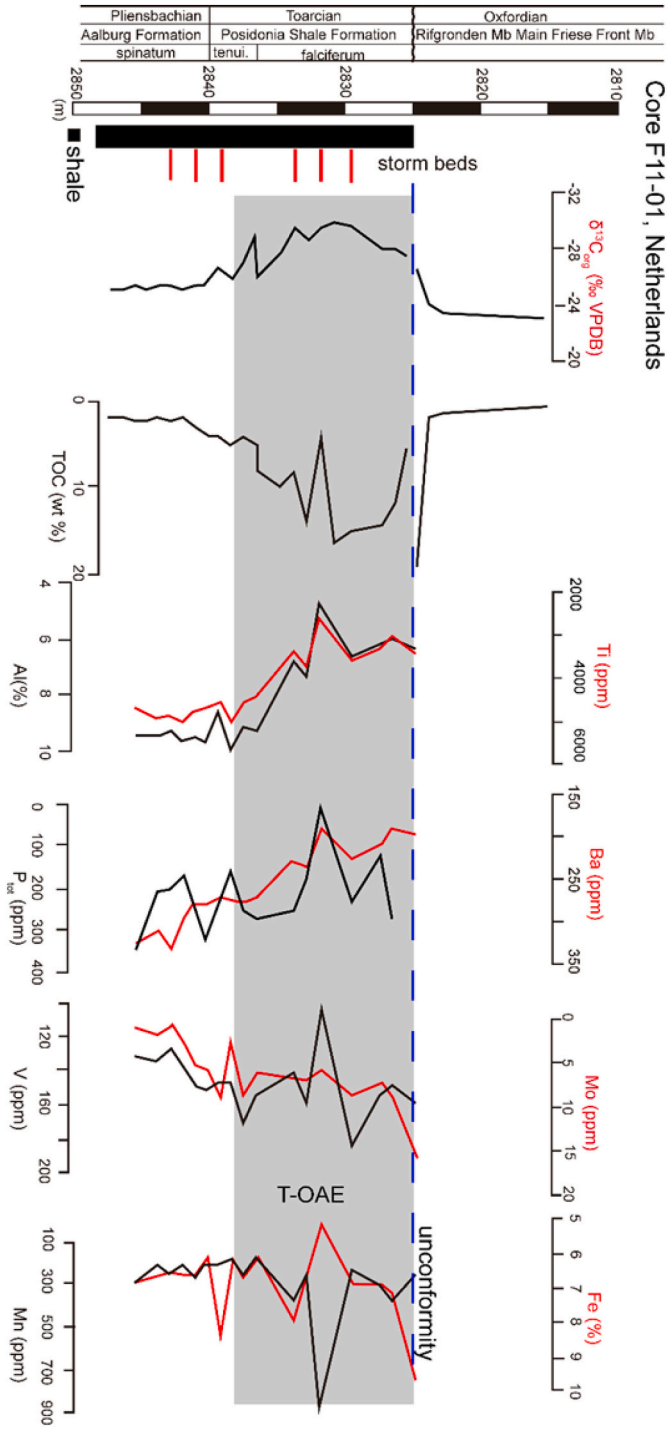

Fig. 8. Lithological and geochemical data of the Core F11–01 section in Dutch Graben (Netherland, number 16 in Fig. 1). The TOAE interval is indicated by the grey field. Storm-related sediment as thin (cm to dm scale) beds showing erosional bases, cross-bedding, normal grading, scour-and-fill structures, and bioturbation. Source: Trabucho-Alexandre et al. (2012).

In the section, the TOAE interval is marked by a negative $\delta^{13}C_{org}$ excursion (ca. –4‰) (Kemp and Izumi, 2014; Chen et al., 2023) (Fig. 10). In the TOAE, low abundance (1–2 wt%) organic matter contains both phytoclasts and amorphous organic matter, although there is a marked rise in phytoclast abundance coeval with the most negative $\delta^{13}C_{org}$ values (Kemp et al., 2019). The TOAE $\delta^{15}N_{tot}$ values are low (−1.2‰ to +1.7‰) with no well-defined secular trends (Fig. 10) (Kemp et al., 2019). Multiple geochemical (e.g., redox-sensitive elements) and ichnofabric proxies suggest mainly oxic settings across the TOAE interval (Chen et al., 2023). Recent Fe species analysis shows higher TOAE Fe_{Py}/Fe_{HR}, which was attributed to Fe^{2+} upwelling from deeper anoxic watermasses (Chen et al., 2023).

3.3.7. *El Penõn (Chile)*

During the Early Jurassic, the El Penõn section within the Andean Basin was deposited on a shallow-marine carbonate-siliciclastic ramp (ca. 30 to 40°S). The Pliensbachian-Toarcian sedimentary interval, belonging to the Montandòn Formation, consists of marly limestone, marl and marly clay (Fantasia et al., 2018b). The TOAE is defined by ammonite and calcareous nannofossil biostratigraphy and carbon-isotope data. During the TOAE, NCIEs (−5‰ for both $\delta^{13}C_{carb}$ and $\delta^{13}C_{org}$), reduced TOC content (<1 wt%), and a shift from marine to terrestrial organic matter (indicated by high HI and low OI) are recorded (Fig. 11) (Fantasia et al., 2018b).

Within the TOAE interval, gravity-flow deposits show well-defined erosive bases, and accumulation of poorly-sorted broken particles reflects increased siliciclastic influx (Fantasia et al., 2018b). Moreover, the combination of broken phosphatized fossils, non-phosphatized grains and the absence of phosphatized sedimentary surfaces also support a gravity-flow origin (Fantasia et al., 2018b). The gravity-flow and tempestitic deposition was associated with sea-level transgression and TOAE NCIE, which is proposed to reflect sediment reworking and winnowing related to high-energy storm activity (Fantasia et al., 2018b).

During the TOAE, enhanced terrestrial influx was associated with lower (rather than higher) chemical index of alteration (CIA) and low kaolinite abundance, which was interpreted to reflect a shift toward more arid climate (Fantasia et al., 2018b). This may have been caused by the southwards migration of the paleo-Intertropical Convergence Zone across southern Gondwana during the TOAE. The decrease of P_{tot} during the TOAE may have been related to reduced nutrient influx with less chemical weathering under a more arid climate, and/or to a dilution effect associated with increased detrital influx (Fantasia et al., 2018b). Moreover, bioturbation, higher hydrodynamics, lower TOC, and redox-sensitive elements suggest mainly oxic settings during the TOAE, which is not favorable for organic-matter preservation. Hg and Hg/TOC enrichment were detected in the TOAE, which may represent signals of distal volcanism (Fig. 11) (Fantasia et al., 2018b).

4. Discussion

4.1. *Storm evidence in marine TOAE records*

TOAE marine records from a range of paleolatitudes and depositional settings exhibit evidence of higher abundance of storm deposits (especially in TOAE NCIE) compared to the pre-TOAE and post-TOAE intervals (e.g., Hesselbo et al., 2007; Ghadeer and Macquaker, 2011; Trabucho-Alexandre et al., 2012; Suan et al., 2013; Han et al., 2018; Izumi et al., 2018; Xu et al., 2018). Widespread storm deposits may be generated by: i) intensified storm activity; or ii) lower storm wave base related to sea-level fall (Remírez and Algeo, 2020b). The latter possibility can be precluded given the known sea-level rise across the TOAE (e.g., Krencker et al., 2015). In the TOAE storm deposits, HCS can reach a height up to 50 cm and wavelengths as much as 4 m, and individual storm beds can be amalgamated (Fig. 12A–C) (Krencker et al., 2015; Han et al., 2018). Associated with HCS are also wave ripples, gutter casts, parallel lamination, climbing ripples, graded bedding and sharp erosive bases (Krencker et al., 2015; Han et al., 2018). Erosional surfaces and normal-graded bedding are also observed in thin sections (Fig. 12D) (Han et al., 2018).

At low latitudes, storm beds in the studied sections are often relatively thick and contain HCS (Fig. 12A–D) (Krencker et al., 2015; Han et al., 2018). Such beds can be either carbonate or siliciclastic in composition, but all show enhanced accumulation of coarser grains and plant debris (Krencker et al., 2015; Han et al., 2018). At higher latitudes

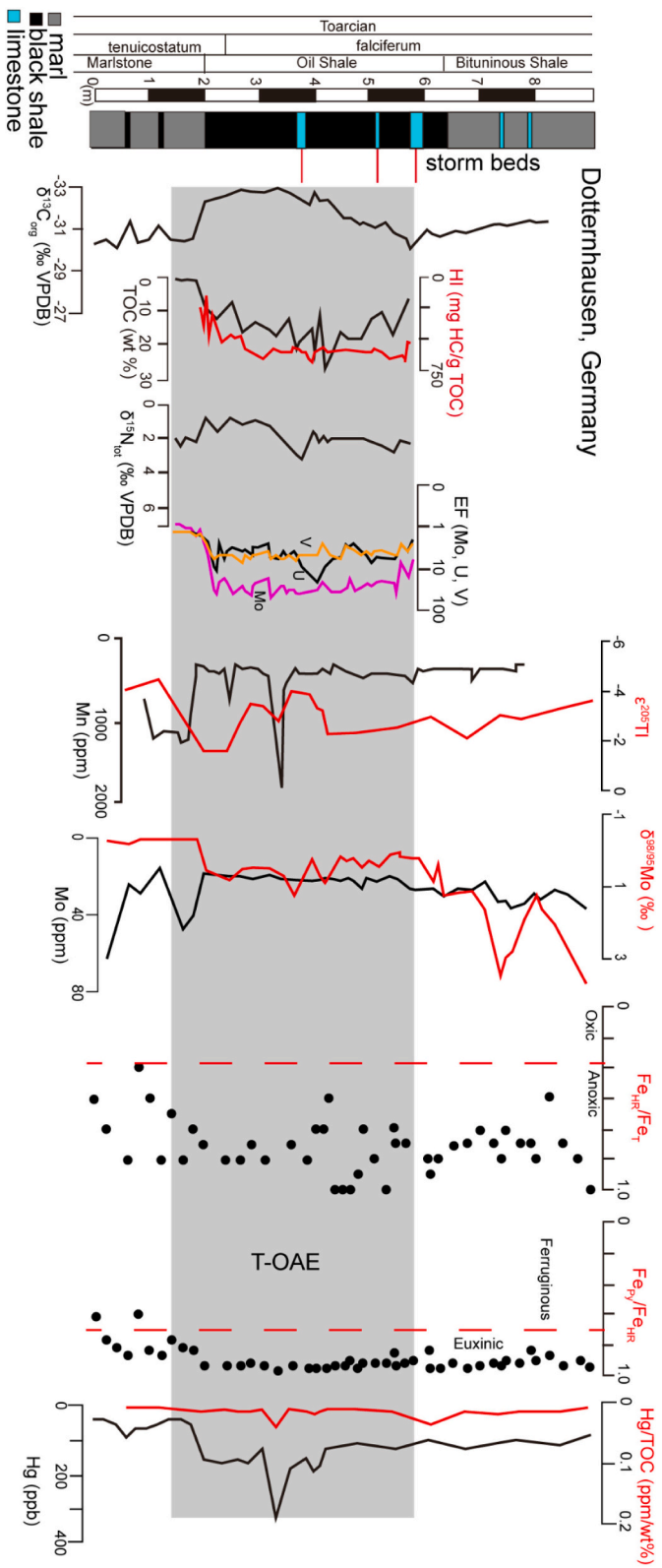

Fig. 9. Lithological and geochemical data of Dotternhausen (Germany, number 14 in Fig. 1). The TOAE interval is indicated by the grey field. Storm-related deposits occur as thin (<1 mm) silty layers with sharp bases within laminated shales. Sources: lithology and storm sedimentation, Röhl et al. (2001); carbon isotope, TOC and HI, Wang et al. (2020, 2021); N isotope, Wang et al. (2021); Mo, U and V, Wang et al. (2021); Mn, Baroni et al. (2018); Mo isotope, Dickson et al. (2017); Tl isotope and Fe species, Them et al. (2018); Hg/TOC, Them et al. (2019).

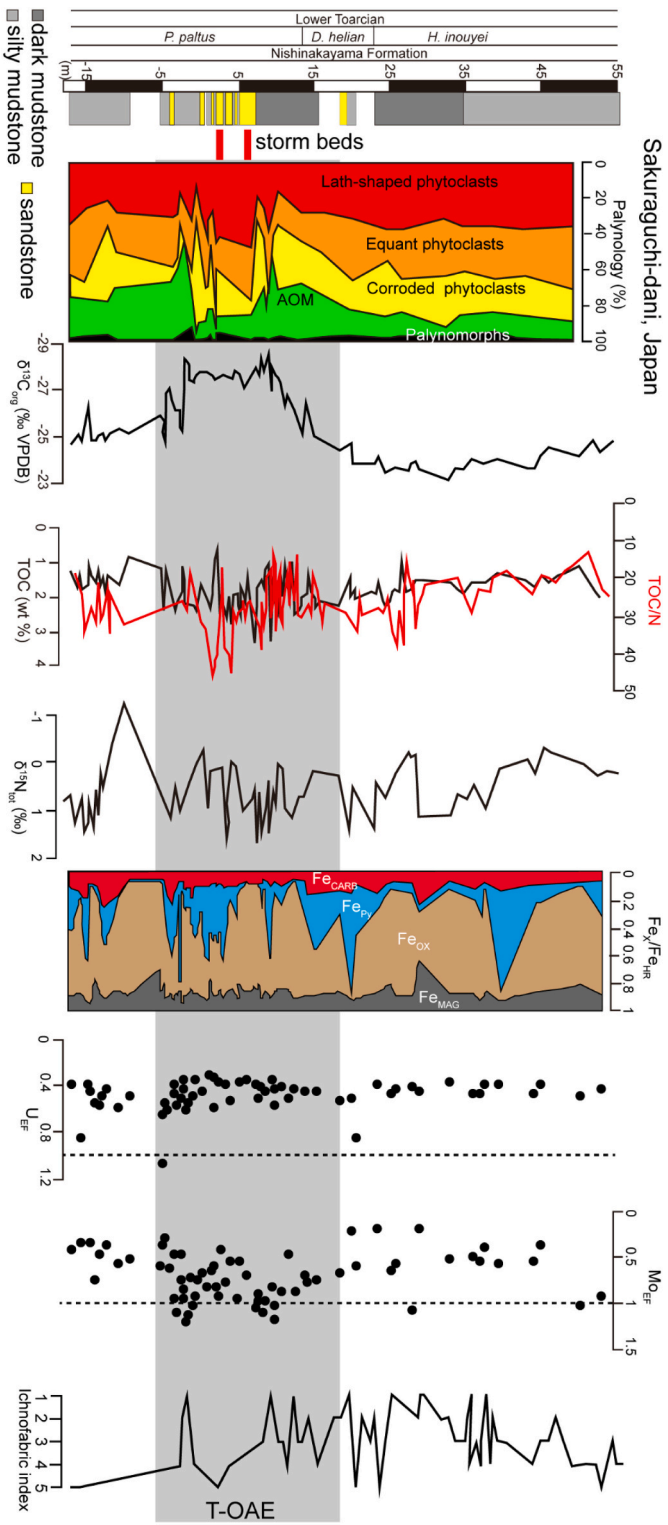

Fig. 10. Lithological, biological and geochemical data of Sakuraguchi-dani (Japan, number 58 in Fig. 1). The TOAE interval is indicated by the grey field. Storm-related deposits occur as dm-m scale sandstone beds showing increased grain size, floated mud clasts, cross-bedding and intense bioturbation. Sources: lithology, storm beds, Kemp and Izumi (2014); palynology, carbon isotope, TOC, TOC/N and N isotope, Kemp et al. (2019); Fe species, U, Mo and ichnofabric index, Chen et al. (2023).

and in restricted low-latitude marine settings, TOAE storm deposits typically occur as thinner beds (or laminae) in both proximal and distal marine settings and were often surrounded by organic-rich shales or mudstones (e.g., Ghadeer and Macquaker, 2011; Trabucho-Alexandre et al., 2012). In the well-studied European epicontinental area, storm sedimentation is hard to observe and occurs within fine-grain sediment (e.g., shale, mudstone) in the cores and/or outcrops. In thin sections, thin beds/lamina (often <10 mm thick) related to storm activity are characterized by sharp and/or erosional bases, normal grading (Fig. 12E), bioturbation and common occurrence of plant debris and/or bioclasts (Fig. 12F) (Ghadeer and Macquaker, 2011; Trabucho-Alexandre et al., 2012; Salem, 2013). Parallel lamination, wave- and current-ripples, gutter casts and intraformational conglomerates are also often observed, while HCS is rarely seen (Ghadeer and Macquaker, 2011; Trabucho-Alexandre et al., 2012). The storm-related thin-bedded sediment is dominated by coarser-grain detrital components and a higher degree of biota colonization and/or bioturbation relative to surrounding sediment (Ghadeer and Macquaker, 2011; Trabucho-Alexandre et al., 2012).

4.2. *Spatially variable storm activity and marine response in TOAE*

Despite the widespread increase in storminess and terrestrial fluxes, the pattern of TOAE storm sedimentation and coupled changes in paleoceanographic conditions were spatially heterogeneous (Figs. 2 to 11; Fig. 13).

In the mid-latitudes, the storm influence at multiple sites Them et al., 2019) was relatively weak and mainly expressed as thin layers (Fig. 12E, F) of intermittent, storm-induced gravity-flow sedimentation (generally lacking HCS) with increased bioturbation and terrestrial influx (Ghadeer and Macquaker, 2011; Xu et al., 2018). At low latitudes, compared with similar sedimentary settings in mid-latitudes, storm sedimentation is characterized by larger thickness and common HCS occurrence. (Fig. 12A to D) (Han et al., 2018; Krencker et al., 2015). Moreover, it has been reported that storm-related sediment redeposition and winnowing became much weaker from low latitude to mid latitude marine realms in TOAE (Suan et al., 2013).

The variation of storm influence between low- and mid-latitudes could be mainly related to latitude-dependent differences in storm activity/mechanisms. As previously suggested, the storms are induced by tropical cyclones and are therefore more intensive at low latitudes (Krencker et al., 2015; Han et al., 2018; Yan et al., 2023). This is supported by the findings of differential storm influence in low- vs. mid-latitude TOAE settings. It is also notable that there is no evidence of T-OAE storm activity above latitudes of 60–70^0. For instance, three Pliensbachian-Toarcian sections from near the paleo-North Pole, representing shallow, intermediate, and deep shelf settings, have been studied in detail, none of which yielded any reported evidence of storm sedimentation (Suan et al., 2011). Thus, there appears to have existed a pattern of weakening storm influence toward higher paleolatitudes. Separately, paleogeographic conditions may be important since relatively weak storm activity in northern Europe (such as at Yorkshire and Dotternhausen) occurred in restricted basins, and thus the degree of storm influence may in part reflect differences between open and restricted marine settings.

The relation between CO_2 change, warming and storminess has been explored using climate modeling for the Early Jurassic, including the TOAE interval (Chandler et al., 1992; Baroni et al., 2018; Yan et al., 2023). For the TOAE, the modeling results show how increasing atmospheric CO_2 and elevated tropical sea surface temperatures will support: i) storm formation and development in tropical oceanic (including Tethys and Panthalassa) areas bounded by the 26.5 °C isotherm ii) two centers of genesis potential in the northwestern and southeastern Tethys between 30°N and 30°S respectively; and iii) weakening storm genesis potential from low to middle-high latitudes (Yan et al., 2023). Interestingly, in the climate modeling of both Baroni et al. (2018) and Yan

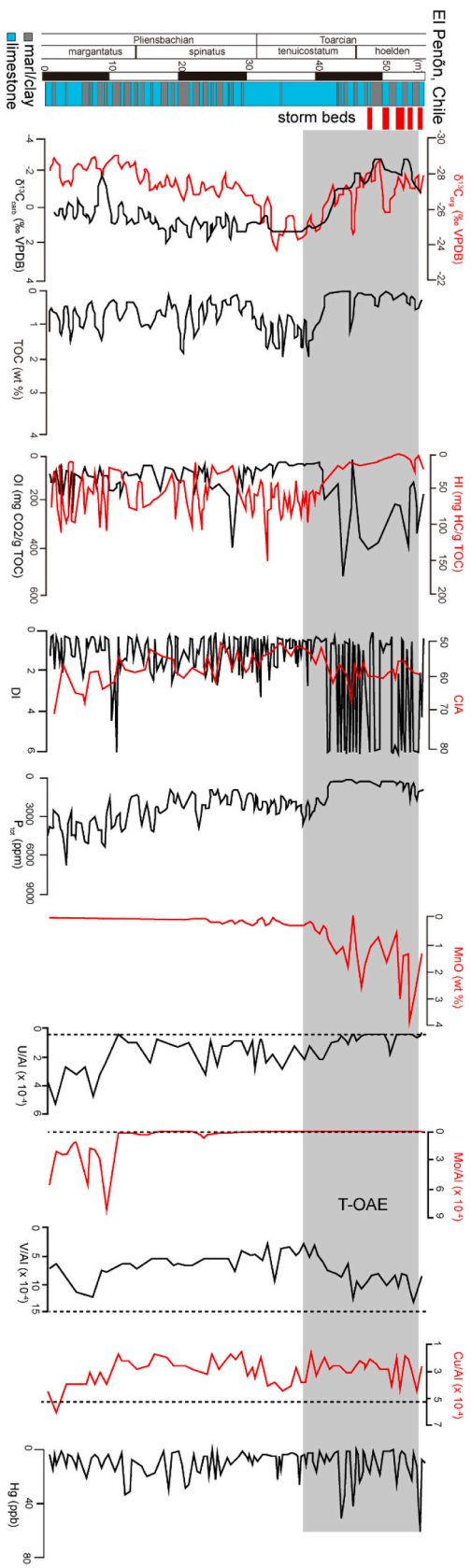

Fig. 11. Lithological and geochemical data of El Penõn (Chile, number 66 in Fig. 1). The TOAE interval is indicated by the grey field. Storm-related sediment is thicker (dm to m scale) bedded and characterized by hummocky cross-stratification, erosive bases, and increased terrestrial debris. Source: Fantasia et al. (2018b).

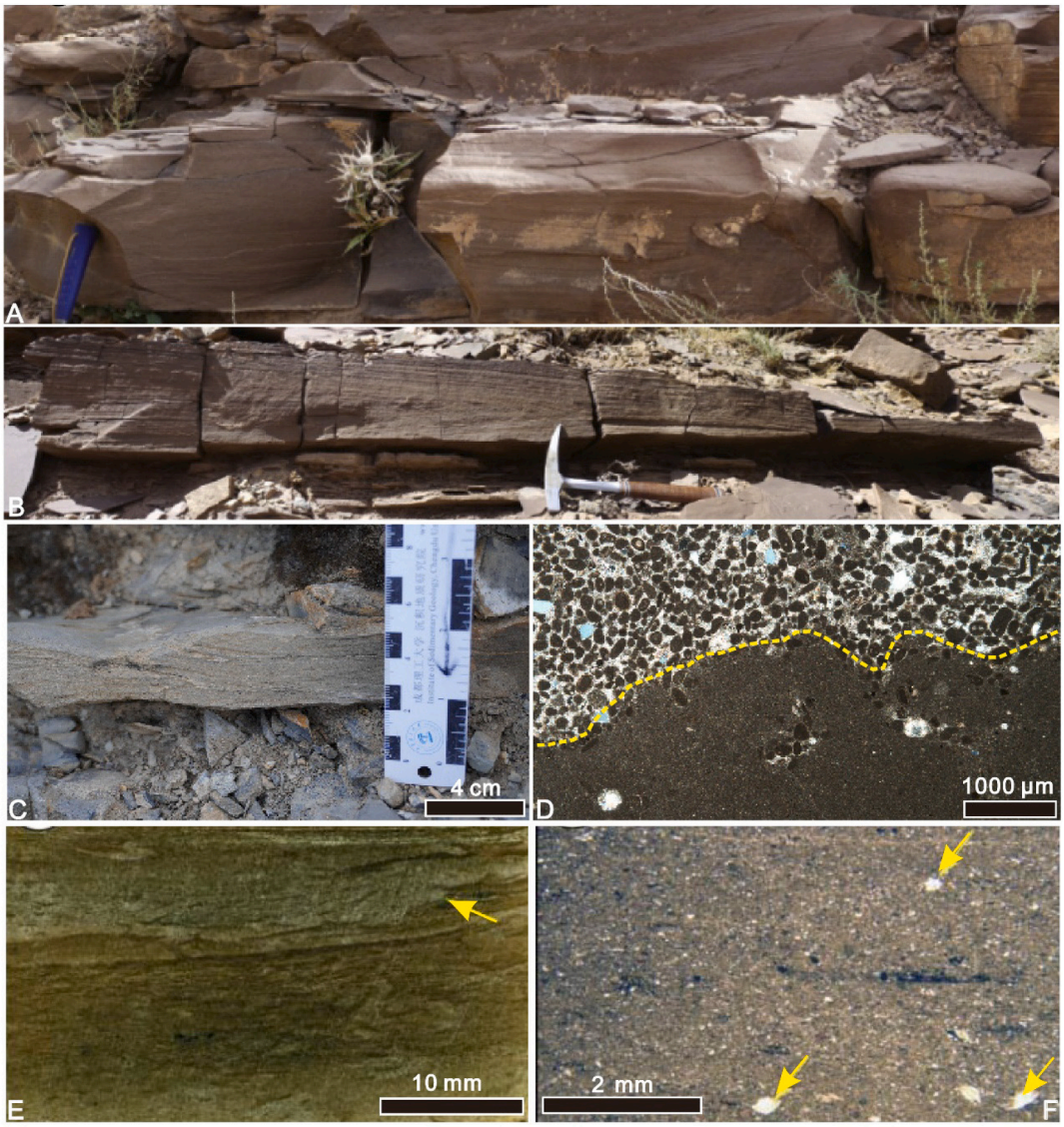

Fig. 12. TOAE storm-related sedimentary features at various sites. (A-B), Hummocky cross-stratification (HCS), TOAE storm bed, Bou Oumadoul and Ouguerd Zegzaoune section, Morocco, Southwestern Tethys, Northern Hemisphere, modified from Krencker et al. (2015); (C) HCS, TOAE storm bed, Nianduo, China (Han et al., 2018), eastern Tethys, Southern Hemisphere; (D) Erosional base (yellow line) with overlying graded bedding, Nianduo, China (Han et al., 2018), eastern Tethys, Southern Hemisphere; (E) Erosional base (yellow arrow) with overlying graded bedding, coastal TOAE section between Staithes and Port Mulgrave, UK, Northwestern Tethys, Northern Hemisphere, modified from Ghadeer and Macquaker (2011); (F) Graded bedding with bioclasts (yellow arrow), coastal TOAE section between Staithes and Port Mulgrave, UK, Southwestern Tethys, Northern Hemisphere, modified from Ghadeer and Macquaker (2011). (For interpretation of the references to colour in this figure legend, the reader is referred to the web version of this article.)

et al. (2023), in the northwestern Tethys Ocean there is an overlap of increased storm genesis potential, enhanced marine oxygenation, and low TOC sediment. Furthermore, the steering flow related to tropical storminess in Yan et al. (2023) shares a similar migration pathway with the Tethyan clockwise gyre in Baroni et al. (2018), which may bring oxic waters and cause brief oxygenation events in the restricted and anoxic basins of west Europe during TOAE.

In the well-studied European epicontinental area of northwestern Tethys, which was associated with weaker storm influence, marine settings were characterized by stronger anoxia (even photic-zone euxinia) and organic-rich (dominated by marine organics with high HI) sedimentation (e.g., Yorkshire, Dotternhausen). Influx of continental freshwater likely promoted water-column stratification, while nutrients from continental runoff and regeneration from anoxic bottom water boosted primary productivity (Brazier et al., 2015; Them et al., 2017b; Baroni et al., 2018; Remírez and Algeo, 2020b). Similar marine environmental features like those of the European epicontinental area have been reported in other restricted, proximal marine areas of northeastern Tethys and back-arc basins adjacent to the southeastern Panthalassic Ocean (Fu et al., 2016; Them et al., 2017b; Al-Suwaidi et al., 2022).

On the other hand, in TOAE open-ocean sections in low-latitude regions, which were associated with stronger storm influence (i.e., Nianduo, Sewa, Peniche, Amellago), there is little evidence for persistent oceanic anoxia (mainly oxic to suboxic facies) and an absence of organic-rich sedimentation. Despite increased terrestrial siliciclastic and nutrient fluxes (Kemp and Izumi, 2014; Krencker et al., 2015; Alnazghah et al., 2022), evidence for water-column stratification and high primary productivity is relatively weak, and preserved organics with low HI and high OI suggest oxidation of marine organics and/or dominance of terrestrial organics (Kemp and Izumi, 2014; Krencker et al., 2015). At the same time, however, marine anoxia has been found in the deep Panthalassic Ocean in Japan (Inuyama area, Kemp et al., 2022a; Chen et al., 2023). The equatorial and deep-ocean open setting of this site may have been well away from the influence of tropical cyclones, and too

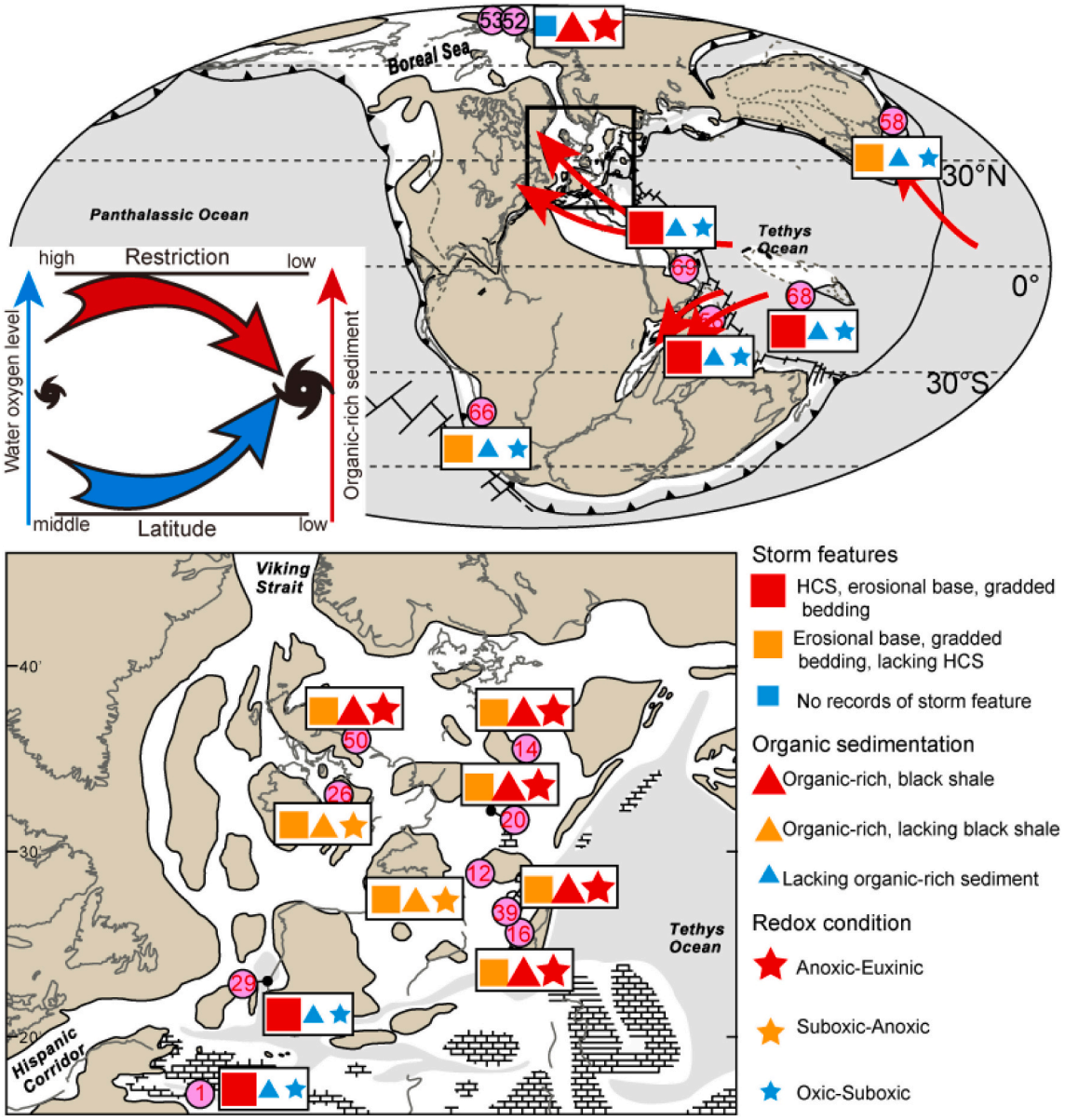

Fig. 13. Summary figure to show spatially variable storminess and marine conditions. Note the covariation of storm intensity, marine redox conditions and marine organic sedimentation. Overall, low-latitude open-marine sites are associated with more intensified storm activity, increased marine oxygenation and reduced marine organic content.

deep to preserve storm signatures in any case.

4.3. *Possible factors influencing heterogeneous TOAE marine responses*

Generally, the TOAE marine response and sedimentation were linked to enhanced continental fluxes under climatic hyperwarming, which led to marine eutrophication, increase of primary productivity and organic-rich deposition (Jenkyns, 2010; Brazier et al., 2015; Them et al., 2017b; Remírez and Algeo, 2020a). The coupling between climate warming, terrigenous influx, and paleoceanographic changes is reliably recorded in the mid-paleolatitude European shelf sections and other proximal and/or restricted marine settings by sufficient sedimentological and geochemical proxies (e.g., Salem, 2013; Fu et al., 2016; Them et al., 2017a, 2017b; Al-Suwaidi et al., 2022). In open-marine settings, enhanced input of terrigenous siliciclastic material has also shown in multiple sections and linked to an accelerated hydrological cycle and/or storm activity (Kemp and Izumi, 2014; Krencker et al., 2015; Alnazghah et al., 2022). However, the elevated continental fluxes were often decoupled from contemporaneous oceanographic changes including marine eutrophication, increase of primary productivity and organic-rich deposition in sedimentary records. In some open-marine sections, reduced TOC and accelerated aerobic degradation of organics has been documented (Fantasia et al., 2018b; Krencker et al., 2020; Alnazghah et al., 2022).

Previous studies have advocated basin restriction and climate variations (humid vs. arid) to account for spatially variable TOAE marine responses. Based on Re, Os and Mo geochemistry, McArthur et al. (2008) suggested watermass restriction in silled basins drove TOAE organic-rich black shale sedimentation and oceanic anoxic events in north-western Europe. However, the deep basinal section in Japan at Inuyama in the Panthalassic Ocean developed organic-rich sedimentation without watermass restriction (Kemp et al., 2022a; Chen et al., 2023). Alternatively, Dera et al. (2009) recognized multiple climate belts during the Pliensbachian-Toarcian interval according to a broad-scale analysis of clay minerals. In the TOAE warm-arid climate belt, continental chemical weathering may have been weak, and weak hydrolytic soil reaction rates

probably did not provide sufficient nutrients for organic-rich sedimentation (Fantasia et al., 2018a). However, open-marine TOAE sections with higher CIA and enhanced continental chemical weathering also display organic-poor sedimentation (Kemp and Izumi, 2014; Fantasia et al., 2019; Fu et al., 2021).

TOAE marine redox conditions are likely to have varied with water depth, especially between well-oxygenated shallower seawater and deeper marine oxygen-deficient oxygen-minimum zones (OMZs) (Chen et al., 2023). However, TOAE open-marine sections showing mainly oxic-suboxic conditions have been distributed in shallow (e.g., marginal marine), middle (e.g., middle-outer ramp) and deep (e.g., hemipelagic) water depths (Kemp and Izumi, 2014; Han et al., 2018; Fantasia et al., 2019; Fu et al., 2021). Further, low $\delta^{15}N_{tot}$ values in open-marine sections (discussed below) support a reduced rather than an expanded OMZ, as might be expected during the TOAE. A possible link between storm intensity and heterogeneous marine response is proposed and discussed below.

4.4. Storm activity and pycnocline variation: a possible control of TOAE marine response

Studies in modern lake and marine settings reveal that storm activity has a key influence on biogeochemistry. In detail, storm action affects aquatic settings by changing continental fluxes, nutrient supply, redox conditions, and ecology (Stal et al., 1999; Chen et al., 2012; Lin et al., 2014; Ni et al., 2016; Planas and Paquet, 2016; Giling et al., 2017; Xu et al., 2019). Specifically, in open-marine areas less influenced by terrestrial influx, strong storm activity mainly expanded the oxygenated region (i.e., reduced OMZ volume) via stronger-than-normal vertical mixing and downwelling, ultimately causing pycnocline deepening in the ocean (Chen et al., 2012; Lin et al., 2014; Ni et al., 2016; Xu et al., 2019). Moreover, a deepened thermocline is related to climate warming and has been reported as a prerequisite to sustain tropical cyclones (Henderson-Sellers et al., 1998). Pycnocline deepening could possibly then lead to: i) enhanced aerobic degradation of organic matter with reduced OMZ; ii) decreased nutrient upwelling from deep ocean into the photic zone, iii) promotion of nitrogen-fixing cyanobacteria and associated calcification in nutrient-depleted conditions, iv) changes in ecology owing to a bloom of cyanobacteria as primary producers (Stal et al., 1999; Lin et al., 2014; Planas and Paquet, 2016; Giling et al., 2017; Xu et al., 2019).

In TOAE open-ocean settings that experienced intensive storm activity, possible pycnocline deepening and reduced OMZ are proposed, similar to that in modern lacustrine and marine settings (Stal et al., 1999; Chen et al., 2012; Lin et al., 2014; Ni et al., 2016; Planas and Paquet, 2016; Giling et al., 2017; Xu et al., 2019). One possible clue for this is from spatial variation of marine $\delta^{15}N_{tot}$ records. The TOAE interval was characterized by enhanced continental weathering and influx, which has been suggested to promote marine primary productivity, enlarge marine OMZ and promote denitrification, hence causing positive $\delta^{15}N$ excursion like modern oceans (Jenkyns et al., 2001; Stüeken, 2013; Ader et al., 2014; Caruthers et al., 2014; Du et al., 2021; Song et al., 2023). However, the TOAE marine $\delta^{15}N_{tot}$ records display both positive and negative excursions of varying magnitudes; reflecting the complexity of nitrogen cycling at this time (Jenkyns et al., 2001; Stüeken, 2013; Ader et al., 2014; Caruthers et al., 2014; Du et al., 2021; Song et al., 2023). In multiple open marine sections of Tethys and Panthalassic Ocean during the TOAE interval, $\delta^{15}N_{tot}$ values show more or less more negative values (especially in the lower TOAE) compared to pre-TOAE interval (Fig. 14). The decrease in $\delta^{15}N$ values is inconsistent with the typical scenarios: increased primary productivity favored by enhanced terrestrial influx in marine settings, would promotes denitrification and lead to high $\delta^{15}N_{tot}$ values (e.g., +4‰ to +10‰ in modern ocean areas) (Jenkyns et al., 2001; Caruthers et al., 2014). Instead, the open-marine negative $\delta^{15}N$ shifts in the TOAE co-occur with storm sedimentation, and correspond to low primary productivity and mainly oxic conditions, as indicated by low TOC, bioturbation and lack of enrichment of redox-sensitive elements (such as Mo, V, U) (Fig. 14).

Possibly, the negative $\delta^{15}N_{tot}$ shifts in the TOAE reflect enhanced nitrogen fixation by cyanobacterial activity under nutrient-depleted conditions with limited nitrate concentrations (Montoya et al., 2002; Knapp et al., 2005; Chang et al., 2019; Du et al., 2021, 2023; Buchanan et al., 2021; Song et al., 2023). Accordingly, enhanced TOAE microbial and abiotic ooid sedimentation and higher marine alkalinity have been recorded in tropical, open oceans in the southern Tethys and eastern Tethys (Trecalli et al., 2012; Han et al., 2018; Krencker et al., 2020; Müller et al., 2020) (Fig. 15). Given elevated continental influx during the TOAE, the nutrient depletion associated with negative $\delta^{15}N_{tot}$ excursion seems strange and counterintuitive, which may point to some other factor(s) inhibiting nutrient upwelling in open marine settings. Although we cannot rule out local influence, this combination of nutrient depletion, cyanobacterial activity, increased alkalinity and ooid sedimentation is consistent with the consequences of pycnocline deepening, which suppresses upwelling of bottom-water nutrients but boosts cyanobacterial activity and biocalcification in nutrient-depleted seawater (Stal et al., 1999; Auderset et al., 2022). Pycnocline deepening is favored by climate warming and increased sea surface temperature, and this may be also favored by storm activity that can efficiently transfer heat and salinity via vertical mixing of ocean water (Chen et al., 2012; Lin et al., 2014; Ni et al., 2016; Xu et al., 2019).

Although only reported in one study from a shallow, open-marine carbonate section (Monte Sorgenza) of the southern Tethys, higher I/Ca ratios support enhanced shallow marine oxygenation during the TOAE, given the positive relation between I/Ca ratios and marine oxygen levels (Lu et al., 2010) (Fig. 14). The storm-related open-marine oxygenation will be favorable for aerobic degradation of organic matter, consistent with the low TOC. Similarly, during the middle Miocene and early Eocene climate warming events, modeling work and nitrogen isotope analysis in marine environments also support lower $\delta^{15}N$ values, pycnocline deepening and higher oxygen levels in the open ocean (Auderset et al., 2022).

In relatively restricted and/or proximal marine settings, like the European epicontinental area during the TOAE, weaker storm influence and more continental influx under a humid and warm climate promoted water-column stratification and a shallower pycnocline depth, favoring nutrient influx from continents and deeper waters fueling higher primary productivity (Jenkyns et al., 2001; Percival et al., 2016). Notably, storm activity at such sites also caused intermittent and short-term watermass oxygenation and benthic colonization events within black shales, which are petrographically known but are perhaps sometimes too short to be captured by geochemical proxies that have relatively long residence times (e.g., Ghadeer and Macquaker, 2011; Trabucho-Alexandre et al., 2012; Suan et al., 2013). Interestingly, with increased restriction, the TOAE marine settings also document increased cyanobacterial/bacterial abundance and a change from positive to negative $\delta^{15}N$ shifts (mainly −1‰ to +3‰) coeval with enhanced watermass anoxia (even photic-zone euxinia) (e.g., Jenkyns et al., 2001; Salem, 2013; Remírez and Algeo, 2020a; Wang et al., 2021) (Fig. 14). This supports enhanced nitrogen-fixing cyanobacterial activity (Wang et al., 2021; Du et al., 2021; Du et al., 2023; Buchanan et al., 2021; Song et al., 2023). Unlike in open-marine settings, nitrogen fixation with increased marine restriction may have been related to quantitative denitrification in low-oxygen (rather than low-nutrient) conditions (Montoya et al., 2002; Knapp et al., 2005; Chang et al., 2019; Buchanan et al., 2021; Wang et al., 2021). In conclusion, apart from basin restriction and climate belt variations, the spatial variation in storm intensity and pycnocline depth may have acted as an important factor influencing marine nutrient cycling, primary productivity, redox conditions and organic-rich sedimentation during the TOAE (Fig. 15).

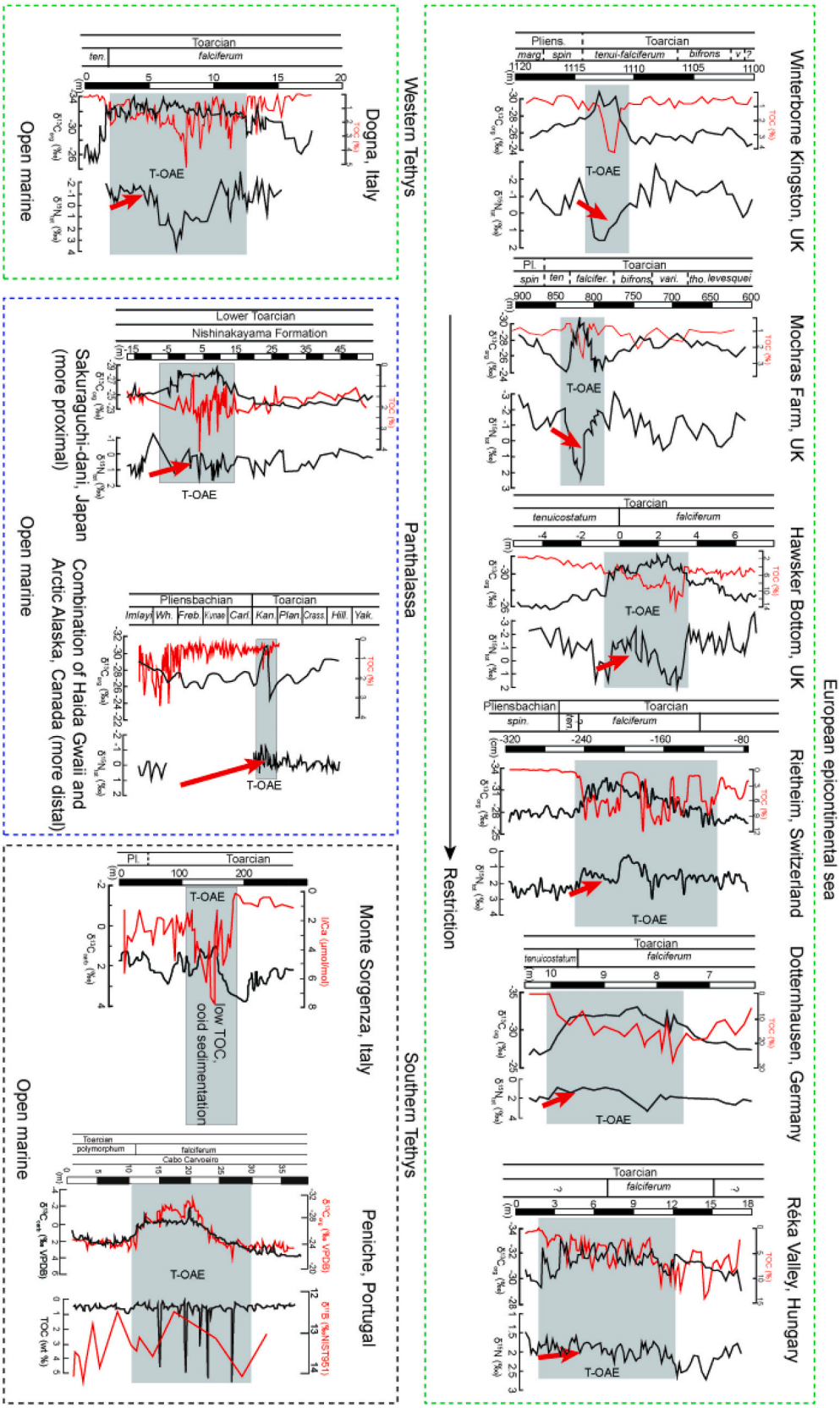

Fig. 14. Nitrogen isotope, I/Ca and B isotope in various marine settings supporting pycnocline deepening in open-marine settings. The TOAE interval is indicated by grey field. Note the various $\delta^{15}N$ excursions (red arrows) associated with both low and high TOC, suggesting increased nitrogen fixation during TOAE. Higher I/Ca and B isotope values indicate higher oxygen and alkalinity during the lower TOAE with storminess. Sources: (1) nitrogen isotope, Jenkyns et al. (2001), Caruthers et al. (2014), Kemp et al. (2019) and Wang et al. (2021); (2) I/Ca, Lu et al. (2010); (3) B isotope, Müller et al. (2020). (For interpretation of the references to colour in this figure legend, the reader is referred to the web version of this article.)

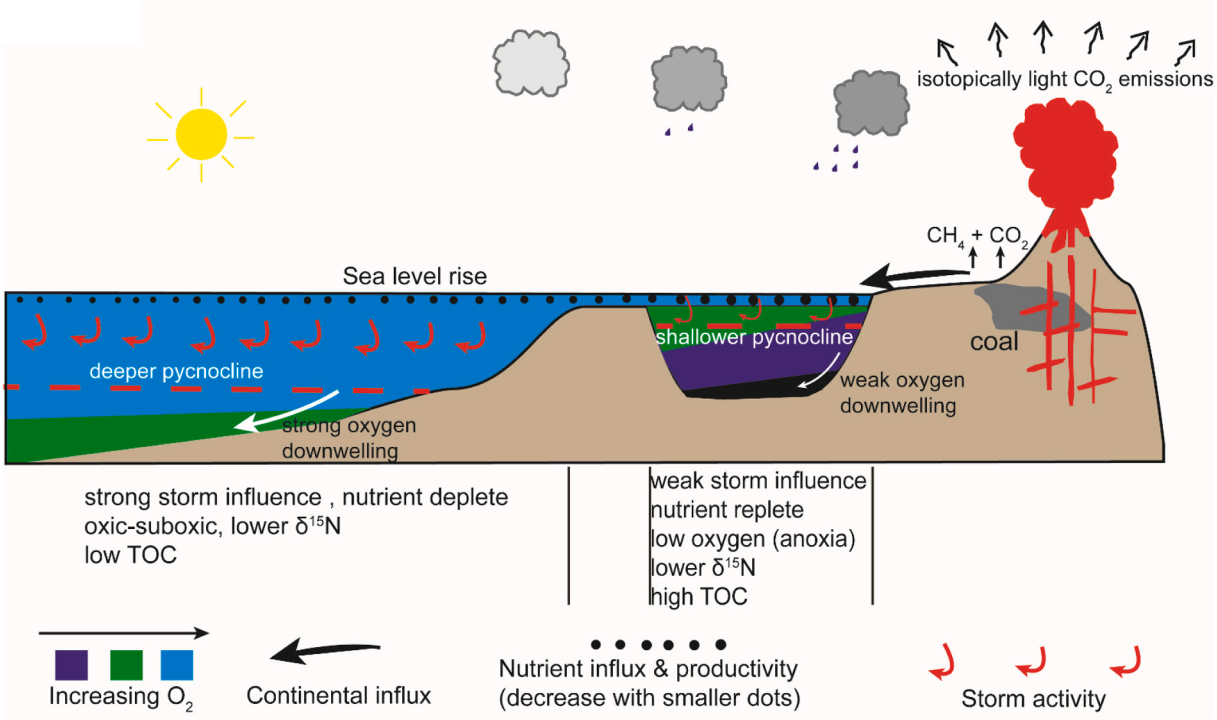

Fig. 15. Sketch illustrating the interaction of storminess, pycnocline depth and marine response during the TOAE. In proximal and/or restricted areas where the storm influence was weak, enhanced continental fluxes led to strong water-column stratification, marine primary productivity increase, watermass anoxia and organic-rich sedimentation. In open-marine settings where the storm influence was strong, the pycnocline deepening caused nutrient-deplete upper ocean settings with oxic conditions and low primary productivity. Both settings are characterized by low $\delta^{15}N$ values. Modified from Remírez and Algeo (2020a).

5. Conclusions

Section that record the Toarcian Oceanic Anoxic Event (TOAE) display obvious spatial heterogeneity rather than universal water-column anoxia and organic-rich sedimentation. On the basis of previous work, this study investigated possibly relationships between enhanced storminess during the TOAE and this spatial heterogeneity. Storm activity during the TOAE is widely reported and commonly caused ocean oxygenation events with variable durations and magnitudes across a range of marine settings. Enhanced storm activity was likely mainly related to intensified tropical cyclones, which were most active at low latitude areas. To the first order, therefore, stronger storm activity at low latitudes could account for the prevalence of oxygenated conditions at such locations. By contrast, weakened storminess could account for the dominance of anoxic and organic-rich facies at mid-latitudes sites. It is proposed that variations in the intensity of storm activity caused spatial variation of ocean pycnocline depths in the TOAE. With more intense storminess, pycnocline deepening would lead to increased oxygenation and reduced nutrient upwelling into surface seawater, therefore favoring oxic water-column conditions and organic-poor sedimentation. This may have contributed to the spatially variable marine responses relative to marine areas with weaker storm activity and predominantly anoxic water, and increased primary productivity and organic-rich sedimentation. Hence, combined with paleogeography and climate, intensified storminess may have acted as an important agent influencing TOAE marine biogeochemical responses. The deep-time relation linking storm and marine responses also gives implications for modern warming world experiencing increased storm frequency.

CRediT authorship contribution statement

Yuzhu Ge: Writing – original draft. **Zhong Han:** Writing – review & editing, Conceptualization. **Thomas J. Algeo:** Writing – review & editing. **David B. Kemp:** Writing – review & editing. **Luya Wu:** Writing – review & editing.

Declaration of competing interest

The authors declare that they have no known competing financial interests or personal relationships that could have appeared to influence the work reported in this paper.

Data availability

Data will be made available on request.

Acknowledgments

This study was financially supported by National Natural Science Foundation of China (No. 42202123, 41888101, 42272116). Thanks for critical comments of the reviewers and editorial guidance of editor M. Zhu.

Appendix A. Supplementary data

Supplementary data to this article can be found online at https://doi.org/10.1016/j.gloplacha.2024.104533.

References

Ader, M., Sansjofre, P., Halverson, G.P., Busigny, V., Trindade, R.I., Kunzmann, M., Nogueira, A.C., 2014. Ocean redox structure across the late Neoproterozoic Oxygenation Event: a nitrogen isotope perspective. Earth Planet. Sci. Lett. 396, 1–13.

Aigner, T., 1982. Calcareous tempestites: Storm-dominated stratification in Upper Muschelkalk limestones (Middle Trias, SW-Germany). In: Einsele, G., Seilacher, A. (Eds.), Cyclic and Event Stratification. Springer Berlin Heidelberg, Berlin, pp. 180–198.

Ajuaba, S., Sachsenhofer, R.F., Bechtel, A., Galasso, F., Gross, D., Misch, D., Schneebeli-Hermann, E., 2022. Biomarker and compound-specific isotope records across the

Toarcian CIE at the Dormettingen section in SW Germany. Int. J. Earth Sci. 111, 1631–1661.
Al-Hussaini, A., Alnazghah, M., Al-Ramadan, K., Fallatah, M., Polo, C., 2021. Asymmetrical wave-dominated siliciclastic shorelines with evidence of along-strike variability of sedimentary processes: a revised interpretation for the Toarcian Marrat red beds, Central Arabia. Mar. Pet. Geol. 126, 104915.
Alnazghah, M., Koeshidayatullah, A., Al-Hussaini, A., Amao, A., Song, H., Al-Ramadan, K., 2022. Evidence for the early Toarcian Carbon Isotope Excursion (T-CIE) from the shallow marine siliciclastic red beds of Arabia. Sci. Rep. 12, 18124.
Al-Suwaidi, A.H., Ruhl, M., Jenkyns, H.C., Damborenea, S.E., Manceñido, M.O., Condon, D.J., Angelozzi, G.N., Kamo, S.L., Storm, M., Riccardi, A.C., Hesselbo, S.P., 2022. New age constraints on the Lower Jurassic Pliensbachian–Toarcian Boundary at Chacay Melehue (Neuquén Basin, Argentina). Sci. Rep. 12, 4975.
Arias, C., 2008. Palaeoceanography and biogeography in the early Jurassic Panthalassa and Tethys oceans. Gondwana Res. 14, 306–315.
Auderset, A., Moretti, S., Taphorn, B., Ebner, P.R., Kast, E., Wang, X.T., Schiebel, R., Sigman, D.M., Haug, G.H., Martínez-García, A., 2022. Enhanced Ocean oxygenation during Cenozoic warm periods. Nature 609, 77–82.
Baroni, R.I., Pohl, A., van Helmond, N.A., Papadomanolaki, N.M., Coe, A.L., Cohen, A.S., Van de Schootbrugge, B., Donnadieu, Y., Slomp, C.P., 2018. Ocean circulation in the Toarcian (early Jurassic): a key control on deoxygenation and carbon burial on the European shelf. PPaleoceanogr. Paleoclimatology 33, 994–1012.
Bhatia, K.T., Vecchi, G.A., Knutson, T.R., Murakami, H., Kossin, J., Dixon, K.W., Whitlock, C.E., 2019. Recent increases in tropical cyclone intensification rates. Nat. Commun. 10, 635.
Bodin, S., Mattioli, E., Fröhlich, S., Marshall, J.D., Boutib, L., Lahsini, S., Redfern, J., 2010. Toarcian carbon isotope shifts and nutrient changes from the Northern margin of Gondwana (High Atlas, Morocco, Jurassic): palaeoenvironmental implications. Palaeogeogr. Palaeoclimatol. Palaeoecol. 297, 377–390.
Bodin, S., Krencker, F.N., Kothe, T., Hoffmann, R., Mattioli, E., Heimhofer, U., Kabiri, L., 2016. Perturbation of the carbon cycle during the late Pliensbachian–early Toarcian: New insight from high-resolution carbon isotope records in Morocco. J. Afr. Earth Sci. 116, 89–104.
Boulila, S., Galbrun, B., Sadki, D., Gardin, S., Bartolini, A., 2019. Constraints on the duration of the early Toarcian T-OAE and evidence for carbon-reservoir change from the High Atlas (Morocco). Glob. Planet. Chang. 175, 113–128.
Brackett, R.S., Bush, D.M., 1986. Sedimentary Characteristics of Modern Storm-Generated Sequences: North Insular Shelf, Puerto Rico. In: Moslow, T.F., Rhodes, E. G. (Eds.), Modern and Ancient Shelf Clastics: A Core Workshop. SEPM Society for Sedimentary Geology, pp. 235–256.
Brazier, J.M., Suan, G., Tacail, T., Simon, L., Martin, J.E., Mattioli, E., Balter, V., 2015. Calcium isotope evidence for dramatic increase of continental weathering during the Toarcian oceanic anoxic event (early Jurassic). Earth Planet. Sci. Lett. 411, 164–176.
Brenchley, P.J., 1989. Storm sedimentation. Geol. Today 5, 133–137.
Buchanan, P.J., Aumont, O., Bopp, L., Mahaffey, C., Tagliabue, A., 2021. Impact of intensifying nitrogen limitation on ocean net primary production is fingerprinted by nitrogen isotopes. Nat. Commun. 12, 6214.
Caruthers, A.H., Smith, P.L., Gröcke, D.R., 2014. The Pliensbachian–Toarcian (early Jurassic) extinction: A north American perspective. In: Keller, G., Kerr, A.C. (Eds.), Volcanism, Impacts, and Mass Extinctions: Causes and Effects. Geol. Soc. Am. Spec. Pap, vol. 505, pp. 225–243.
Chandler, M.A., Rind, D., Ruedy, R., 1992. Pangean climate during the early Jurassic: GCM simulations and the sedimentary record of paleoclimate. Geol. Soc. Am. Bull. 104, 543–559.
Chang, C., Hu, W., Wang, X., Huang, K.J., Yang, A., Zhang, X., 2019. Nitrogen isotope evidence for an oligotrophic shallow ocean during the Cambrian Stage 4. Geochim. Cosmochim. Acta 257, 49–67.
Charbonnier, G., Adatte, T., Föllmi, K.B., Suan, G., 2020. Effect of intense weathering and postdepositional degradation of organic matter on Hg/TOC proxy in organic-rich sediments and its implications for deep-time investigations. Geochem. Geophys. Geosyst. 21 e2019GC008707.
Chen, J., Ni, X., Mao, Z., Wang, Y., Liang, L., Gong, F., 2012. Remote sensing and buoy-based effect analysis of typhoon on hypoxia off the Changjiang (Yangtze) Estuary. In: Remote Sensing of the Ocean, Sea Ice, Coastal Waters, and Large Water Regions 2012, vol. 8532. SPIE, pp. 257–264.
Chen, W., Kemp, D.B., He, T., Newton, R.J., Xiong, Y., Jenkyns, H.C., Izumi, K., Cho, T., Huang, C., Poulton, S.W., 2023. Shallow-and deep-ocean Fe cycling and redox evolution across the Pliensbachian–Toarcian boundary and Toarcian Oceanic Anoxic Event in Panthalassa. Earth Planet. Sci. Lett. 602, 117959.
Cohen, A.S., Coe, A.L., Harding, S.M., Schwark, L., 2004. Osmium isotope evidence for the regulation of atmospheric CO_2 by continental weathering. Geology 32, 157–160.
Cope, J.C., 1984. The Mesozoic history of Wales. Proc. Geol. Assoc. 95, 373–385.
Correia, V.F., Riding, J.B., Duarte, L.V., Fernandes, P., Pereira, Z., 2017. The palynological response to the Toarcian Oceanic Anoxic Event (early Jurassic) at Peniche, Lusitanian Basin, western Portugal. Mar. Micropaleontol. 137, 46–63.
Dera, G., Donnadieu, Y., 2012. Modeling evidences for global warming, Arctic seawater freshening, and sluggish oceanic circulation during the early Toarcian anoxic event. Paleoceanography 27, PA2211.
Dera, G., Pellenard, P., Neige, P., Deconinck, J.F., Dommergues, J.L., 2009. Distribution of clay minerals in early Jurassic Peritethyan seas: Palaeoclimatic significance inferred from multiproxy comparisons. Palaeogeogr. Palaeoclimatol. Palaeoecol. 271, 39–51.
Dickson, A.J., Gill, B.C., Ruhl, M., Jenkyns, H.C., Porcelli, D., Idiz, E., Lyons, T.W., van den Boorn, S.H., 2017. Molybdenum-isotope chemostratigraphy and paleoceanography of the Toarcian Oceanic Anoxic Event (early Jurassic). Paleoceanography 32, 813–829.
Donnelly, J.P., Hawkes, A.D., Lane, P., MacDonald, D., Shuman, B.N., Toomey, M.R., van Hengstum, P.J., Woodruff, J.D., 2015. Climate forcing of unprecedented intense-hurricane activity in the last 2000 years. Earth's Future 3, 49–65.
Du, Y., Song, H., Tong, J., Algeo, T.J., Li, Z., Song, H., Huang, J., 2021. Changes in productivity associated with algal-microbial shifts during the early Triassic recovery of marine ecosystems. Geol. Soc. Am. Bull. 133, 362–378.
Du, Y., Song, H., Grasby, S.E., Xing, T., Song, H., Tian, L., Chu, D., Wu, Y., Dal Corso, J., Algeo, T.J., Tong, J., 2023. Recovery from persistent nutrient-N limitation following the Permian–Triassic mass extinction. Earth Planet. Sci. Lett. 602, 117944.
Duarte, L.V., 1997. Facies analysis and sequential evolution of the Toarcian–Lower Aalenian series in the Lusitanian Basin (Portugal). Comun. Inst. Geol. Mineiro 83, 65–94.
Einsele, G., 2000. Sedimentary Basin: Evolution, Facies and Sediment Budget, second ed. Springer, Heidelberg.
Emanuel, K.A., 1987. The dependence of hurricane intensity on climate. Nature 326, 483–485.
Fantasia, A., Föllmi, K.B., Adatte, T., Spangenberg, J.E., Montero-Serrano, J.C., 2018a. The early Toarcian oceanic anoxic event: Paleoenvironmental and paleoclimatic change across the Alpine Tethys (Switzerland). Glob. Planet. Chang. 162, 53–68.
Fantasia, A., Föllmi, K.B., Adatte, T., Bernárdez, E., Spangenberg, J.E., Mattioli, E., 2018b. The Toarcian oceanic anoxic event in southwestern Gondwana: an example from the Andean Basin, northern Chile. J. Geol. Soc. Lond. 175, 883–902.
Fantasia, A., Adatte, T., Spangenberg, J.E., Font, E., Duarte, L.V., Föllmi, K.B., 2019. Global versus local processes during the Pliensbachian–Toarcian transition at the Peniche GSSP, Portugal: a multi-proxy record. Earth Sci. Rev. 198, 102932.
Font, E., Duarte, L.V., Dekkers, M.J., Remazeilles, C., Egli, R., Spangenberg, J.E., Fantasia, A., Ribeiro, J., Gomes, E., Mirão, J., Adatte, T., 2022. Rapid light carbon releases and increased aridity linked to Karoo–Ferrar magmatism during the early Toarcian oceanic anoxic event. Sci. Rep. 12, 4342.
French, K.L., Sepúlveda, J., Trabucho-Alexandre, J., Gröcke, D.R., Summons, R.E., 2014. Organic geochemistry of the early Toarcian oceanic anoxic event in Hawsker Bottoms, Yorkshire, England. Earth Planet. Sci. Lett. 390, 116–127.
Fu, X., Wang, J., Feng, X., Wang, D., Chen, W., Song, C., Zeng, S., 2016. Early Jurassic carbon-isotope excursion in the Qiangtang Basin (Tibet), the eastern Tethys: Implications for the Toarcian Oceanic anoxic event. Chem. Geol. 442, 62–72.
Fu, X., Wang, J., Wen, H., Song, C., Wang, Z., Zeng, S., Feng, X., Wei, H., 2021. A Toarcian Ocean Anoxic Event record from an open-ocean setting in the eastern Tethys: Implications for global climatic change and regional environmental perturbation. Sci. China Earth Sci. 64, 1860–1872.
Ghadeer, S.G., Macquaker, J.H., 2011. Sediment transport processes in an ancient mud-dominated succession: a comparison of processes operating in marine offshore settings and anoxic basinal environments. J. Geol. Soc. Lond. 168, 1121–1132.
Giling, D.P., Nejstgaard, J.C., Berger, S.A., Grossart, H.P., Kirillin, G., Penske, A., Lentz, M., Casper, P., Sareyka, J., Gessner, M.O., 2017. Thermocline deepening boosts ecosystem metabolism: evidence from a large-scale lake enclosure experiment simulating a summer storm. Glob. Chang. Biol. 23, 1448–1462.
Golonka, J., 2007. Late Triassic and early Jurassic palaeogeography of the world. Palaeogeogr. Palaeoclimatol. Palaeoecol. 244, 297–307.
Han, Z., Hu, X., Li, J., Garzanti, E., 2016. Jurassic carbonate microfacies and relative sea-level changes in the Tethys Himalaya (southern Tibet). Palaeogeogr. Palaeoclimatol. Palaeoecol. 456, 1–20.
Han, Z., Hu, X., Kemp, D.B., Li, J., 2018. Carbonate-platform response to the Toarcian Oceanic Anoxic Event in the southern hemisphere: implications for climatic change and biotic platform demise. Earth Planet. Sci. Lett. 489, 59–71.
Han, Z., Hu, X., Hu, Z., Jenkyns, H.C., Su, T., 2022a. Geochemical evidence from the Kioto Carbonate Platform (Tibet) reveals enhanced terrigenous input and deoxygenation during the early Toarcian. Glob. Planet. Chang. 215, 103887.
Han, Z., Hu, X., He, T., Newton, R.J., Jenkyns, H.C., Jamieson, R.A., Franceschi, M., 2022b. Early Jurassic long-term oceanic sulfur-cycle perturbations in the Tibetan Himalaya. Earth Planet. Sci. Lett. 578, 117261.
Hansen, J., 46 Co-Authors, 2007. Dangerous human-made interference with climate: a GISS modelE study. Atmos. Chem. Phys. 7, 2287–2312.
Henderson-Sellers, A., Zhang, H., Berz, G., Emanuel, K., Gray, W., Landsea, C., Holland, G., Lighthill, J., Shieh, S., Webster, P., McGuffie, K., 1998. Tropical cyclones and global climate change: a post-IPCC assessment. Bull. Am. Meteorol. Soc. 79, 19–38.
Hermoso, M., Minoletti, F., Le Callonnec, L., Jenkyns, H.C., Hesselbo, S.P., Rickaby, R.E., Renard, M., de Rafélis, M., Emmanuel, L., 2009. Global and local forcing of early Toarcian seawater chemistry: a comparative study of different paleoceanographic settings (Paris and Lusitanian basins). Paleoceanography 24, PA4208.
Hesselbo, S.P., Jenkyns, H.C., Duarte, L.V., Oliveira, L.C., 2007. Carbon-isotope record of the early Jurassic (Toarcian) Oceanic Anoxic Event from fossil wood and marine carbonate (Lusitanian Basin, Portugal). Earth Planet. Sci. Lett. 253, 455–470.
Izumi, K., Kemp, D.B., Itamiya, S., Inui, M., 2018. Sedimentary evidence for enhanced hydrological cycling in response to rapid carbon release during the early Toarcian oceanic anoxic event. Earth Planet. Sci. Lett. 481, 162–170.
Jenkyns, H.C., 2010. Geochemistry of oceanic anoxic events. Geochem. Geophys. Geosyst. 11, Q03004.
Jenkyns, H.C., Gröcke, D.R., Hesselbo, S.P., 2001. Nitrogen isotope evidence for water mass denitrification during the early Toarcian (Jurassic) oceanic anoxic event. Paleoceanography 16, 593–603.
Jiang, S., Song, H., Kemp, D.B., Dai, X., Liu, X., 2020. Two pulses of extinction of larger benthic foraminifera during the Pliensbachian-Toarcian and early Toarcian environmental crises. Palaeogeogr. Palaeoclimatol. Palaeoecol. 560, 109998.
Johnson, M.A., Belderson, R.H., 1969. The tidal origin of some vertical sedimentary changes in epicontinental seas. J. Geol. 77, 353–357.

Kemp, D.B., Izumi, K., 2014. Multiproxy geochemical analysis of a Panthalassic margin record of the early Toarcian oceanic anoxic event (Toyora area, Japan). Palaeogeogr. Palaeoclimatol. Palaeoecol. 414, 332–341.
Kemp, D.B., Baranyi, V., Izumi, K., Burgess, R.D., 2019. Organic matter variations and links to climate across the early Toarcian oceanic anoxic event (T-OAE) in Toyora area, Southwest Japan. Palaeogeogr. Palaeoclimatol. Palaeoecol. 530, 90–102.
Kemp, D.B., Suan, G., Fantasia, A., Jin, S., Chen, W., 2022a. Global organic carbon burial during the Toarcian oceanic anoxic event: patterns and controls. Earth Sci. Rev. 231, 104086.
Kemp, D.B., Chen, W., Cho, T., Algeo, T.J., Shen, J., Ikeda, M., 2022b. Deep-ocean anoxia across the Pliensbachian-Toarcian boundary and the Toarcian Oceanic Anoxic Event in the Panthalassic Ocean. Glob. Planet. Chang. 212, 103782.
Kiehl, J.T., Zarzycki, C.M., Shields, C.A., Rothstein, M.V., 2021. Simulated changes to tropical cyclones across the Paleocene-Eocene thermal Maximum (PETM) boundary. Palaeogeogr. Palaeoclimatol. Palaeoecol. 572, 110421.
Knapp, A.N., Sigman, D.M., Lipschultz, F., 2005. N isotopic composition of dissolved organic nitrogen and nitrate at the Bermuda Atlantic Time-series Study site. Glob. Biogeochem. Cycles 19, GB1018.
Knutson, T.R., Tuleya, R.E., 2004. Impact of CO2-induced warming on simulated hurricane intensity and precipitation: Sensitivity to the choice of climate model and convective parameterization. J. Clim. 17, 3477–3495.
Kossin, J.P., Knapp, K.R., Olander, T.L., Velden, C.S., 2020. Global increase in major tropical cyclone exceedance probability over the past four decades. Proc. Natl. Acad. Sci. USA 117, 11975–11980.
Kreisa, R.D., Bambach, R.K., 1982. The role of storm processes in generating shell beds in Paleozoic shelf environments. In: Einsele, G., Seilacher, A. (Eds.), Cyclic and Event Stratification. Springer, Heidelberg, pp. 200–207.
Krencker, F.N., Bodin, S., Suan, G., Heimhofer, U., Kabiri, L., Immenhauser, A., 2015. Toarcian extreme warmth led to tropical cyclone intensification. Earth Planet. Sci. Lett. 425, 120–130.
Krencker, F.N., Fantasia, A., Danisch, J., Martindale, R., Kabiri, L., El Ouali, M., Bodin, S., 2020. Two-phased collapse of the shallow-water carbonate factory during the late Pliensbachian–Toarcian driven by changing climate and enhanced continental weathering in the Northwestern Gondwana Margin. Earth Sci. Rev. 208, 103254.
Kullberg, J.C., Olóriz, F., Marques, B., Caetano, P., Rocha, R.B., 2001. Flat pebble conglomerates: a local marker for early Jurassic seismicity related to syn-rift tectonics in the Sesimbra area (Lusitanian Basin, Portugal). Sediment. Geol. 139, 49–70.
Kumar, N., Sanders, J.E., 1976. Characteristics of shoreface storm deposits: modern and ancient examples. J. Sediment. Res. 46, 145–162.
Landwehrs, J., Feulner, G., Petri, S., Sames, B., Wagreich, M., 2021. Investigating Mesozoic climate trends and sensitivities with a large ensemble of climate model simulations. Paleoceanography 36 p.e2020PA004134.
Lin, J., Tang, D., Alpers, W., Wang, S., 2014. Response of dissolved oxygen and related marine ecological parameters to a tropical cyclone in the South China Sea. Adv. Space Res. 53, 1081–1091.
Lu, Z., Jenkyns, H.C., Rickaby, R.E., 2010. Iodine to calcium ratios in marine carbonate as a paleo-redox proxy during oceanic anoxic events. Geology 38, 1107–1110.
Mailliot, S., Mattioli, E., Bartolini, A., Baudin, F., Pittet, B., Guex, J., 2009. Late Pliensbachian–Early Toarcian (Early Jurassic) environmental changes in an epicontinental basin of NW Europe (Causses area, central France): a micropaleontological and geochemical approach. Palaeogeogr. Palaeoclimatol. Palaeoecol. 273, 346–364.
Masselink, G., Heteren, V.S., 2014. Response of wave-dominated and mixed-energy barriers to storms. Mar. Geol. 352, 321–347.
Mattioli, E., Pittet, B., 2004. Spatial and temporal distribution of calcareous nannofossils along a proximal–distal transect in the lower Jurassic of the Umbria–Marche Basin (Central Italy). Palaeogeogr. Palaeoclimatol. Palaeoecol. 205, 295–316.
McArthur, J.M., Algeo, T.J., Van de Schootbrugge, B., Li, Q., Howarth, R.J., 2008. Basinal restriction, black shales, Re-Os dating, and the early Toarcian (Jurassic) oceanic anoxic event. Paleoceanography 23, PA4217.
Montoya, J.P., Carpenter, E.J., Capone, D.G., 2002. Nitrogen fixation and nitrogen isotope abundances in zooplankton of the oligotrophic North Atlantic. Limnol. Oceanogr. 47, 1617–1628.
Müller, T., Jurikova, H., Gutjahr, M., Tomašových, A., Schlögl, J., Liebetrau, V., Duarte, L.V., Milovský, R., Suan, G., Mattioli, E., Pittet, B., 2020. Ocean acidification during the early Toarcian extinction event: evidence from boron isotopes in brachiopods. Geology 48, 1184–1188.
Myrow, P.M., Southard, J.B., 1996. Tempestite deposition. J. Sediment. Res. 66, 875–887.
Newton, R.J., Reeves, E.P., Kafousia, N., Wignall, P.B., Bottrell, S.H., Sha, J.G., 2011. Low marine sulfate concentrations and the isolation of the European epicontinental sea during the early Jurassic. Geology 39, 7–10.
Ni, X., Huang, D., Zeng, D., Zhang, T., Li, H., Chen, J., 2016. The impact of wind mixing on the variation of bottom dissolved oxygen off the Changjiang Estuary during summer. J. Mar. Syst. 154, 122–130.
Nichols, G.J., 2009. Sedimentology and Stratigraphy. John Wiley and Sons, New York.
Nielsen, S.G., Goff, M., Hesselbo, S.P., Jenkyns, H.C., LaRowe, D.E., Lee, C.T.A., 2011. Thallium isotopes in early diagenetic pyrite–a paleoredox proxy? Geochim. Cosmochim. Acta 75, 6690–6704.
Nordt, L., Breecker, D., White, J., 2022. Jurassic greenhouse ice-sheet fluctuations sensitive to atmospheric CO2 dynamics. Nat. Geosci. 15, 54–59.
Pearce, C.R., Cohen, A.S., Coe, A.L., Burton, K.W., 2008. Molybdenum isotope evidence for global ocean anoxia coupled with perturbations to the carbon cycle during the early Jurassic. Geology 36, 231–234.
Percival, L.M.E., Witt, M.L.I., Mather, T.A., Hermoso, M., Jenkyns, H.C., Hesselbo, S.P., Al-Suwaidi, A.H., Storm, M.S., Xu, W., Ruhl, M., 2015. Globally enhanced mercury deposition during the end-Pliensbachian extinction and Toarcian OAE: A link to the Karoo–Ferrar Large Igneous Province. Earth Planet. Sci. Lett. 428, 267–280.
Percival, L.M., Cohen, A.S., Davies, M.K., Dickson, A.J., Hesselbo, S.P., Jenkyns, H.C., Leng, M.J., Mather, T.A., Storm, M.S., Xu, W., 2016. Osmium isotope evidence for two pulses of increased continental weathering linked to early Jurassic volcanism and climate change. Geology 44, 759–762.
Pittet, B., Suan, G., Lenoir, F., Duarte, L.V., Mattioli, E., 2014. Carbon isotope evidence for sedimentary discontinuities in the lower Toarcian of the Lusitanian Basin (Portugal): sea level change at the onset of the Oceanic Anoxic Event. Sediment. Geol. 303, 1–14.
Planas, D., Paquet, S., 2016. Importance of climate change-physical forcing on the increase of cyanobacterial blooms in a small, stratified lake. J. Limnol. 75, 201–214.
Remírez, M.N., Algeo, T.J., 2020a. Carbon-cycle changes during the Toarcian (early Jurassic) and implications for regional versus global drivers of the Toarcian oceanic anoxic event. Earth Sci. Rev. 209, 103283.
Remírez, M.N., Algeo, T.J., 2020b. Paleosalinity determination in ancient epicontinental seas: a case study of the T-OAE in the Cleveland Basin (UK). Earth Sci. Rev. 201, 103072.
Röhl, H.J., Schmid-Röhl, A., Oschmann, W., Frimmel, A., Schwark, L., 2001. The Posidonia Shale (lower Toarcian) of SW-Germany: an oxygen-depleted ecosystem controlled by sea level and palaeoclimate. Palaeogeogr. Palaeoclimatol. Palaeoecol. 165, 27–52.
Ruebsam, W., Müller, T., Kovács, J., Pálfy, J., Schwark, L., 2018. Environmental response to the early Toarcian carbon cycle and climate perturbations in the northeastern part of the West Tethys shelf. Gondwana Res. 59, 144–158.
Ruebsam, W., Reolid, M., Schwark, L., 2020. $\delta^{13}C$ of terrestrial vegetation records Toarcian CO_2 and climate gradients. Sci. Rep. 10, 117.
Salem, N.E., 2013. Geochemical Characterisation of the Pliensbachian-Toarcian Boundary During the Onset of the Toarcian Oceanic Anoxic Event. North Yorkshire, UK. Master's Thesis. Newcastle University, UK.
Sellwood, B.W., Jenkyns, H.G., 1975. Basins and swells and the evolution of an epeiric sea: (Pliensbachian–Bajocian of Great Britain). J. Geol. Soc. Lond. 131, 373–388.
Slater, S.M., Twitchett, R.J., Danise, S., Vajda, V., 2019. Substantial vegetation response to early Jurassic global warming with impacts on oceanic anoxia. Nat. Geosci. 12, 462–467.
Sobel, A.H., Camargo, S.J., Hall, T.M., Lee, C.Y., Tippett, M.K., Wing, A.A., 2016. Human influence on tropical cyclone intensity. Science 353, 242–246.
Song, H., An, Z., Ye, Q., Stüeken, E.E., Li, J., Hu, J., Algeo, T.J., Tian, L., Chu, D., Song, H., Xiao, S., 2023. Mid-latitudinal habitable environment for marine eukaryotes during the waning stage of the Marinoan snowball glaciation. Nat. Commun. 14, 1564.
Stal, L.J., Staal, M., Villbrandt, M., 1999. Nutrient control of cyanobacterial blooms in the Baltic Sea. Aquat. Microb. Ecol. 18, 165–173.
Stüeken, E.E., 2013. A test of the nitrogen-limitation hypothesis for retarded eukaryote radiation: Nitrogen isotopes across a Mesoproterozoic basinal profile. Geochim. Cosmochim. Acta 120, 121–139.
Suan, G., Mattioli, E., Pittet, B., Mailliot, S., Lécuyer, C., 2008. Evidence for major environmental perturbation prior to and during the Toarcian (early Jurassic) oceanic anoxic event from the Lusitanian Basin, Portugal. Paleoceanography 23, PA1202.
Suan, G., Nikitenko, B.L., Rogov, M.A., Baudin, F., Spangenberg, J.E., Knyazev, V.G., Glinskikh, L.A., Goryacheva, A.A., Adatte, T., Riding, J.B., Föllmi, K.B., Pittet, B., Mattioli, E., Lécuver, C., 2011. Polar record of early Jurassic massive carbon injection. Earth Planet. Sci. Lett. 312, 102–113.
Suan, G., Rulleau, L., Mattioli, E., Sucheras-Marx, B., Rousselle, B., Pittet, B., Vincent, P., Martin, J.E., Lena, A., Spangenberg, J.E., Foellmi, K.B., 2013. Palaeoenvironmental significance of Toarcian black shales and event deposits from southern Beaujolais, France. Geol. Mag. 150, 728–742.
Swift, D.J., Hudelson, P.M., Brenner, R.L., Thompson, P., 1987. Shelf construction in a foreland basin: storm beds, shelf sandbodies, and shelf-slope depositional sequences in the Upper cretaceous Mesaverde Group, Book Cliffs, Utah. Sedimentology 34, 423–457.
Them II, T.R., Gill, B.C., Caruthers, A.H., Gröcke, D.R., Tulsky, E.T., Martindale, R.C., Poulton, T.P., Smith, P.L., 2017a. High-resolution carbon isotope records of the Toarcian Oceanic Anoxic Event (early Jurassic) from North America and implications for the global drivers of the Toarcian carbon cycle. Earth Planet. Sci. Lett. 459, 118–126.
Them II, T.R., Gill, B.C., Selby, D., Gröcke, D.R., Friedman, R.M., Owens, J.D., 2017b. Evidence for rapid weathering response to climatic warming during the Toarcian Oceanic Anoxic Event. Sci. Rep. 7, 5003.
Them II, T.R., Gill, B.C., Caruthers, A.H., Gerhardt, A.M., Gröcke, D.R., Lyons, T.W., Marroquin, S.M., Nielsen, S.G., Alexandre, J.P.T., Owens, J.D., 2018. Thallium isotopes reveal protracted anoxia during the Toarcian (early Jurassic) associated with volcanism, carbon burial, and mass extinction. Proc. Natl. Acad. Sci. USA 115, 6596–6601.
Them II, T.R., Jagoe, C.H., Caruthers, A.H., Gill, B.C., Grasby, S.E., Gröcke, D.R., Yin, R., Owens, J.D., 2019. Terrestrial sources as the primary delivery mechanism of mercury to the oceans across the Toarcian Oceanic Anoxic Event (early Jurassic). Earth Planet. Sci. Lett. 507, 62–72.
Trabucho-Alexandre, J., Dirkx, R., Veld, H., Klaver, G., de Boer, P.L., 2012. Toarcian black shales in the Dutch Central Graben: record of energetic, variable depositional conditions during an oceanic anoxic event. J. Sediment. Res. 82, 104–120.
Trecalli, A., Spangenberg, J., Adatte, T., Föllmi, K.B., Parente, M., 2012. Carbonate platform evidence of ocean acidification at the onset of the early Toarcian oceanic anoxic event. Earth Planet. Sci. Lett. 357, 214–225.

Tucker, M.E., Wright, V.P., 1990. Carbonate Sedimentology. Blackwell Science Ltd, Oxford.
Ullmann, C.V., Szücs, D., Jiang, M., Hudson, A.J., Hesselbo, S.P., 2022. Geochemistry of macrofossil, bulk rock and secondary calcite in the Early Jurassic strata of the Llanbedr (Mochras Farm) drill core, Cardigan Bay Basin, Wales, UK. J. Geol. Soc. Lond. 179 jgs2021–018.
van Breugel, Y., Baas, M., Schouten, S., Mattioli, E., Sinninghe Damsté, J.S., 2006. Isorenieratane record in black shales from the Paris Basin, France: Constraints on recycling of respired CO_2 as a mechanism for negative carbon isotope shifts during the Toarcian oceanic anoxic event. Paleoceanography 21, PA4220.
Vichi, M., Eayrs, C., Alberello, A., Bekker, A., Bennetts, L., Holland, D., de Jong, E., Joubert, W., MacHutchon, K., Messori, G., Mojica, J.F., 2019. Effects of an explosive polar cyclone crossing the Antarctic marginal ice zone. Geophys. Res. Lett. 46, 5948–5958.
Wang, Y.Q., Wu, C.C., 2004. Current understanding of tropical cyclone structure and intensity changes–a review. Meteorog. Atmos. Phys. 87, 257–278.
Wang, Y.F., Ossa Ossa, F., Wille, M., Schurr, S., Saussele, M.E., Schmid-Röhl, A., Schoenberg, R., 2020. Evidence for local carbon-cycle perturbations superimposed on the Toarcian carbon isotope excursion. Geobiology 18, 682–709.
Wang, Y.F., Ossa Ossa, F., Spangenberg, J.E., Wille, M., Schoenberg, R., 2021. Restricted oxygen-deficient basins on the northern European epicontinental shelf across the Toarcian carbon isotope excursion interval. Paleoceanogr. Paleoclimatol. 36 e2020PA004207.
Ware, B., Jourdan, F., Timms, N.E., 2023. The Ferrar Continental Flood Basalt: a ~1.6 Ma long duration evidenced by high-precision $^{40}Ar/^{39}Ar$ ages suggest a potential role in the Pliensbachian-Toarcian extinction event. Earth Planet. Sci. Lett. 622, 118369.
Wignall, P.B., Newton, R.J., Little, C.T., 2005. The timing of paleoenvironmental change and cause-and-effect relationships during the early Jurassic mass extinction in Europe. Am. J. Sci. 305, 1014–1032.
Xu, W., Ruhl, M., Jenkyns, H.C., Leng, M.J., Huggett, J.M., Minisini, D., Ullmann, C.V., Riding, J.B., Weijers, J.W., Storm, M.S., Percival, L.M., 2018. Evolution of the Toarcian (early Jurassic) carbon-cycle and global climatic controls on local sedimentary processes (Cardigan Bay Basin, UK). Earth Planet. Sci. Lett. 484, 396–411.
Xu, H., Tang, D., Sheng, J., Liu, Y., Sui, Y., 2019. Study of dissolved oxygen responses to tropical cyclones in the Bay of Bengal based on Argo and satellite observations. Sci. Total Environ. 659, 912–922.
Yan, Q., Wei, T., Korty, R.L., Kossin, J.P., Zhang, Z., Wang, H., 2016. Enhanced intensity of global tropical cyclones during the mid-Pliocene warm period. Proc. Natl. Acad. Sci. USA 120, 12963–12967.
Yan, Q., Li, X., Kemp, D.B., Guo, J., Zhang, Z., Hu, Y., 2023. Elevated atmospheric CO_2 drove an increase in tropical cyclone intensity during the early Toarcian hyperthermal. Proc. Natl. Acad. Sci. USA 120, e2301018120.